# Rotaxane or Pseudorotaxane? Effects of Small Structural Variations on the Deslipping Kinetics of Rotaxanes with Stopper Groups of Intermediate Size

**Ansgar Affeld,[a] Gosia M. Hübner,[a] Christian Seel,[a] and Christoph A. Schalley*[a]**

**Keywords:** Arrhenius kinetics / Eyring theory / Rotaxanes / Slipping synthesis / Supramolecular chemistry / Template synthesis

Three series of rotaxanes have been synthesized variously by slipping synthesis, in which axis and wheel are melted in admixture, by recognition of amide groups inside the macrocyclic wheel, or by an anionic template method, in which the stoppering phenolates are hydrogen bonded to the wheel and then joined by reaction with a semi-axle. The 3,5-di-*tert*-butylphenyl stopper used for most of these rotaxanes is large enough to permit their isolation, but still allows the wheel to deslip from the axle under appropriate conditions. The deslipping activation parameters for all rotaxanes are derived from $^1$H NMR kinetic measurements and have been evaluated from the Arrhenius equation as well as according to Eyring theory. Small structural variations give rise to surprising effects on the activation parameters. Firstly, in some examples, the axle length affects the deslipping barrier, although the size complementarity of stopper and wheel remain unchanged. Secondly, stopper flexibility has an important influence on the deslipping rate. Thirdly, exchange of a carbonamide for a sulfonamide in the wheel significantly reduces the entropic costs of the deslipping, resulting in a pronounced deslipping rate enhancement. Fourthly, intramolecular hydrogen bonding within the wheel decelerates deslipping by a factor of more than $10^4$.

## Introduction

During the last decade, the chemistry of mechanically linked molecules[1] – rotaxanes, catenanes, and knots[2] – has received fresh impetus from the development of efficient template methods for the synthesis of these compounds.[3] It is not, however, only their synthetic availability that has promoted increasing interest in these species. The discovery of naturally occurring, catenated DNA rings,[1b,4] knotted proteins,[5] and the rotaxane-like ATP synthase[6] and flagellum motors in bacteria[7] have also shed new light on their artificial analogs and their properties. Topological chirality[8] and the development of molecular machines based on rotaxanes and catenanes[9] are two of the most intriguing aspects of these species. Many other functional properties such as electron transfer or energy transfer from one stopper to the other,[10] the quenching of luminescence in self-assembled pseudorotaxanes,[11] photoswitchability of the catenanes' ring geometry,[12] electric conductance through polyrotaxanes,[13] and the implementation of logic functions at the molecular level[14] have been studied intensely.

Here, we present results from deslipping experiments that give insight into those features of the rotaxanes that relate to molecular mobility. In the deslipping reaction (Scheme 1), one of the stoppers slides through the wheel, abolishing the mechanical bond between axle and wheel and liberating the free components, but without cleaving any covalent bond. This process has several aspects which are of interest. Firstly, the height of the activation barrier is determined by the relative sizes of the inner diameter of the wheel and the outer boundary of the stoppers.[15] Kinetic measurements of the deslipping of a series of rotaxanes with, for example, the same wheel and different axles can thus be used to measure the effective size requirements for different stoppers. A similar approach making use of half-life time measurements has recently been applied to rotaxanes with dendritic stoppers.[16] Secondly, depending on conditions such as temperature and solvent, there exists a region of intermediate stability[17] between rotaxanes and pseudorotaxanes.[18] While the former are stable entities, due to the presence of bulky end groups attached to the axle, the latter do not form inclusion complexes in the absence of attractive forces, due to the entropic preference for the free species. Between these two extremes, rotaxanes with stoppers of medium size exist as metastable species, the stability of which strongly depends on the environment. Deslipping experiments provide insights into the requirements necessary to render a rotaxane metastable. Thirdly, deslipping is the *retro* reaction corresponding to the slipping synthesis.[19] Study of it consequently yields more detailed information about the slipping synthesis and might be useful for its further refinement. Finally, how does a wheel move along the axle? This question has been addressed with respect to molecular shuttles,[20] rotaxanes that bear two "stations" in the axle, as well as to the related process of circumrotation in catenanes.[21] A kinetic analysis of the deslipping represents another approach to this question, since the entropy of activation should be affected by the nature of the shuttling process.

[a] Kekulé-Institut für Organische Chemie und Biochemie der Universität,
Gerhard-Domagk-Strasse 1, 53121 Bonn, Germany
E-mail: c.schalley@uni-bonn.de

  1434–193X/01/0815–2877 $ 17.50+.50/0 


Scheme 1. Schematic representation of the deslipping process and illustration of the working hypothesis

## Results and Discussion

### The Working Hypothesis and its Implications

As a starting point for our investigation, we will use the following model. An *idealized* rotaxane in its simplest representation (Scheme 1) is a structure built out of three different subunits: a cyclic wheel, a straight and slender axle, and a spherical, bulky stopper at each of the two ends of the axle. The bond between axle and wheel is purely mechanical; dethreading is hampered only by the stoppers, and not by additional forces between axle and wheel. In this view, movement of the wheel along the axle can be regarded as a unidimensional diffusion process, which may result in successful deslippage upon collision of the wheel with one of the stoppers. This process is a unimolecular reaction, and accordingly follows first order kinetics.

$$k = k_\infty e^{-\frac{E_A}{RT}} \quad (1)$$

$$\ln k = \ln k_\infty - \frac{E_A}{RT} \quad (2)$$

This model has some implications for the activation parameters $k_\infty$ and $E_A$, as derived from the *Arrhenius* equation [Equations (1) and (2)]. The energy of activation, $E_A$, represents the barrier of the rate-determining step of a reaction. For the deslipping process, it may reasonably be expected that this value is determined by the passage of the bulkiest part of the stopper. In contrast, the slender central part of the axle should not be associated with high barriers of any kind and so would not be expected to affect $E_A$. Accordingly, different rotaxanes with the same stoppers and wheels, but with different central axle moieties should be subject to the same barrier $E_A$. The frequency factor $k_\infty$ instead encompasses the entropic effects of the deslipping reaction. In particular, for closely related rotaxanes with different axle lengths, one would expect to find frequency factors decreasing with increasing axle length, since a longer axle results in an increased time needed by the wheel to shuttle from one end of the axle to the other. Thus, a lower number of collisions of the wheel with the two stoppers should result for longer axles, also reducing the preexponential factor.

$$k = \frac{k_B T}{h} e^{-\frac{\Delta G^{\neq}}{RT}} = \frac{k_B T}{h} e^{-\frac{\Delta H^{\neq} - T\Delta S^{\neq}}{RT}} \quad (3)$$

$$\ln \frac{k}{T} = \ln \frac{k_B}{h} + \frac{\Delta S^{\neq}}{R} - \frac{\Delta H^{\neq}}{RT} \quad (4)$$

Another approach to the kinetic parameters of the deslipping reaction is the determination of $\Delta G^{\ddagger}$, $\Delta H^{\ddagger}$, and $\Delta S^{\ddagger}$ according to the *Eyring* theory [Equations (3) and (4), $k_B$ is the Boltzmann constant, $h$ the Planck quantum]. The two methods of evaluation differ somewhat, each having its own advantages and disadvantages. For comparative purposes, both were used to evaluate the data summarized in Table 1. Although the two approaches do not produce identical results in an absolute sense, the trends follow the same patterns and it seems reasonable to discuss the data jointly.

Before discussion of several structural variations and their effects on deslipping kinetics, let us consider one representative example of a kinetics experiment. Figure 1 shows the $^1$H NMR spectra of **Rot1@2** after several time intervals at 384 K. It can clearly be seen that the signals of the rotaxane are becoming smaller and those of the free components appearing. In particular, the signals for $H^c$ and $H^d$ in the axle's central part can easily be followed, because they are significantly shifted to higher field in the rotaxane ($\delta$ = 6.69 and 6.95) than in the free axle ($\delta$ = 7.38 and 7.63), due to the anisotropy of the aromatic rings incorporated in the wheel. On the basis of these measurements at four different temperatures, it is possible to determine the rate constants $k$ (Figure 2, a) and evaluate the kinetic parameters in Arrhenius (Figure 2, b) and Eyring (Figure 2, c) plots.

### Different Axle Central Units

With respect to our simple model, let us first consider the effects of different axle central units on the deslipping kinetics of rotaxanes with the same 3,5-di-*tert*-butylphenyl stoppers and the same tetralactam wheel **2**. Scheme 2 summarizes the data obtained for **Rot1@2**−**Rot4@2**, together with the structures of their wheel and axles. In all of these rotaxanes, the central units differ not in length but in flexibility. While **Rot1@2** has some additional degrees of freedom due to the axle's single bonds, rotation of these bonds is certainly reduced with the introduction of the amide bond, with its partial double bond character, and of the double bond in the other two rotaxanes. Furthermore, **Rot3@2** is capable of hydrogen bonding to the wheel with at least two, and more probably three hydrogen bonds − as implied by studies of the much better binding abilities[22] of secondary amides versus tertiary ones and the presence of three hydrogen bonds in X-ray structures of similar rotaxanes.[23] However, the kinetic data do not show large differences in this series of rotaxanes. There seems to be a trend in the entropic terms ($k_\infty$ and $\Delta S^{\ddagger}$), with lower axle flexibility resulting in a lower activation entropy, but the effects are so small that we may consider **Rot1@2**−**Rot4@2** to be more or less the same in terms of their kinetic deslippage parameters.

This picture changes, however, when axles of different lengths are considered (Scheme 3), in that a longer axle indeed results in a decreased value of $k_\infty$, as predicted by our simple model. Not very pronounced in the first series (**Rot4@2**−**Rot6@2**), which was studied in [$D_7$]DMF, the effect becomes obvious for the structurally related rotaxanes

Table 1. Kinetic parameters derived from evaluation of $^1$H NMR kinetic experiments according to the Arrhenius and Eyring theories, together with half-lifes at 333 K and axle lengths obtained from molecular modeling of the most extended conformations, using the Sybyl force field as implemented in the Spartan program[33]

| | $E_A$ [kJ mol$^{-1}$] | $k_\infty$ [MHz] | $\Delta G^\ddagger$ (298 K) [kJ mol$^{-1}$] | $\Delta H^\ddagger$ [kJ mol$^{-1}$] | $\Delta S^\ddagger$ [J K$^{-1}$ mol$^{-1}$] | $t1/2$ (333 K) [h] | l [Å] |
|---|---|---|---|---|---|---|---|
| **Rot1@2** [a] | 84 | 26 | 94 | 81 | −45 | 111 | 14.5 |
| **Rot3@2** [a] | 81 | 16 | 93 | 78 | −49 | 61 | 14.5 |
| **Rot4@2** [a] | 77 | 4 | 92 | 68 | −80 | 58 | 14.6 |
| **Rot4@2** [b] | 63 | 0.1 | 88 | 60 | −93 | 23 | 14.6 |
| **Rot5@2** [a] | 83 | 42 | 92 | 81 | −39 | 48 | 10.6 |
| **Rot6@2** [a] | 77 | 2 | 93 | 74 | −64 | 115 | 16.9 |
| **Rot7@2** [c] | 104 | 48300 | 96 | 101 | 18 | 82 | 10.0 |
| **Rot8@2** [c] | 98 | 12050 | 93 | 95 | 7 | 38 | 14.1 |
| **Rot9@2** [c] | 88 | 1530 | 88 | 85 | −10 | 8 | 16.0 |
| **Rot9@2** [d] | 85 | 848 | 82 | 87 | −15 | 5 | 16.0 |
| **Rot10@2′** [c] | 77 | 470 | 80 | 74 | −19 | < 1 | 10.0 |
| **Rot11@2′** [c] | 79 | 130 | 85 | 76 | −30 | 4 | 16.0 |
| **Rot4@12** [a] | 75 | 920 | 76 | 68 | −26 | < 0.5 | 14.6 |
| **Rot5@12** [a] | 82 | 4940 | 75 | 75 | 0 | < 0.5 | 10.6 |
| **Rot3@13** [a] | 134 | 50 | 142 | 130 | −40 | >10$^6$ | 14.5 |
| **Rot3@14** [a] | No deslipping observed | | | | | | |

[a] Solvent: [D$_7$]dimethylformamide. − [b] Solvent: [D$_8$]tetrahydrofuran. − [c] Solvent: [D$_2$]tetrachloroethane. − [d] Solvent: [D]chloroform.

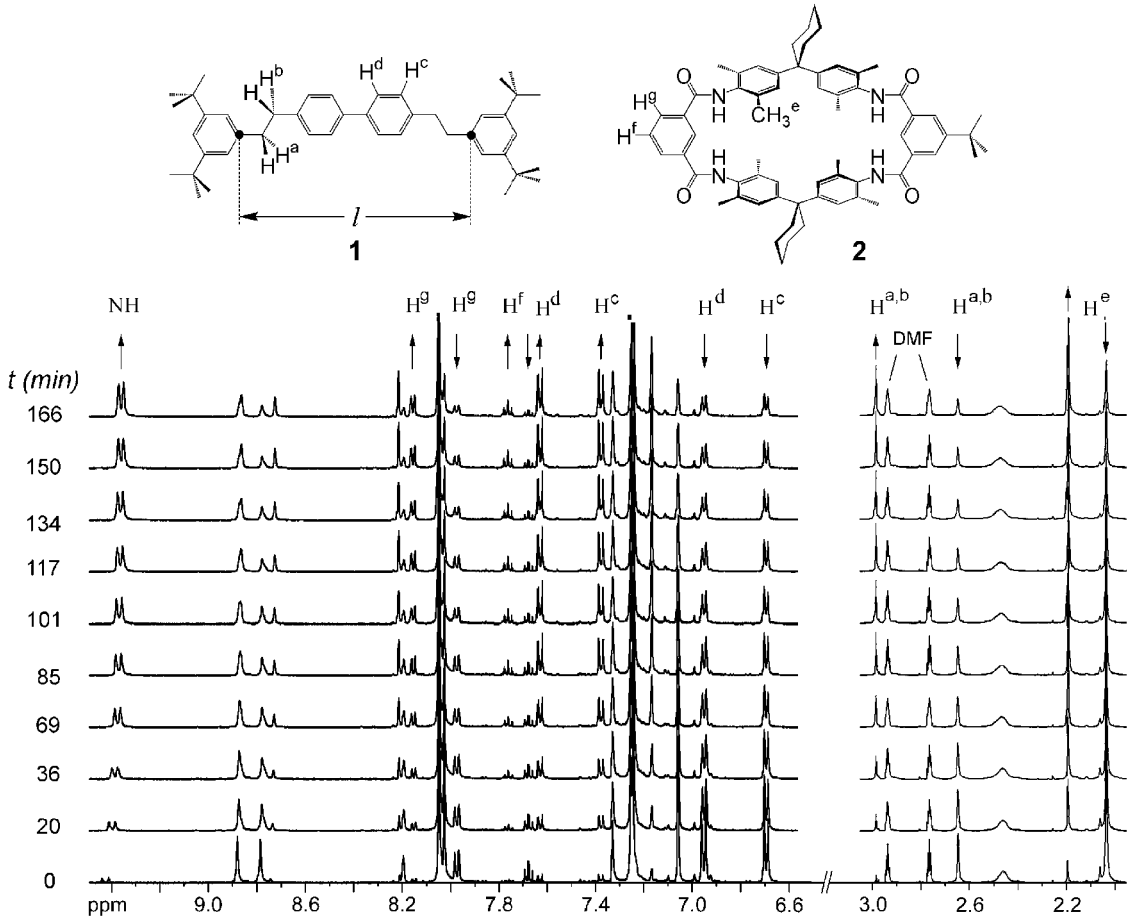


Figure 1. $^1$H NMR kinetics experiment with **Rot1@2** at a temperature of 384 K (increasing time intervals from bottom to top). The arrows indicate the decreasing signals of the rotaxane and the growing signals of the free components. The signal assignment is given in the formulae, together with the definition of axle length used in the text and Table 1

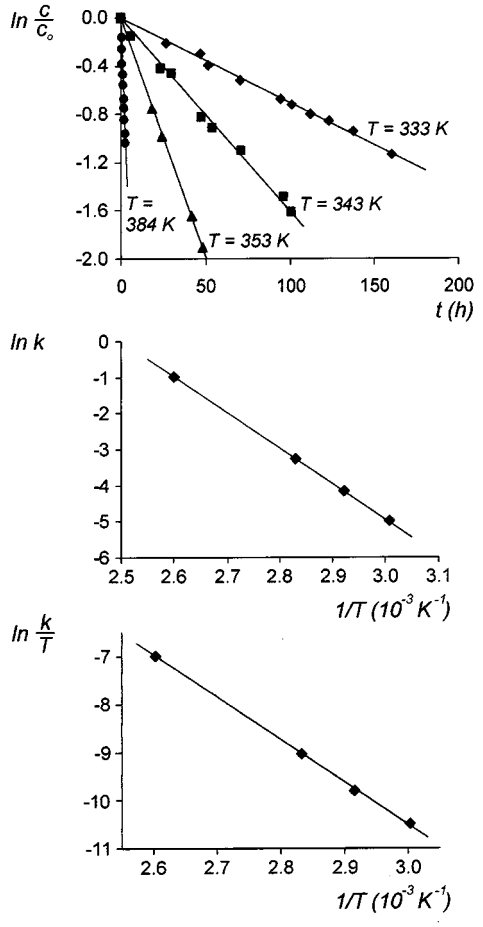


Figure 2. From top to bottom: (a) Determination of rate constants for **Rot1@2** at four different temperatures, (b) Arrhenius plot for the evaluation of $E_A$ and $k_\infty$. (c) Eyring plot for the determination of $\Delta G^\ddagger$, $\Delta H^\ddagger$, and $\Delta S^\ddagger$

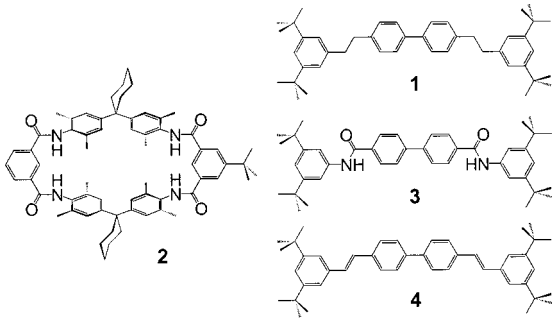


| | $E_A$ [kJ mol$^{-1}$] | $k_\infty$ [MHz] | $\Delta H^\ddagger$ [kJ mol$^{-1}$] | $\Delta S^\ddagger$ [J K$^{-1}$ mol$^{-1}$] | $t_{1/2}$ (333 K) [h] |
|---|---|---|---|---|---|
| Rot1@2 | 84 | 26 | 81 | -45 | 111 |
| Rot3@2 | 81 | 16 | 78 | -49 | 61 |
| Rot4@2 | 77 | 4 | 68 | -80 | 58 |

Scheme 2. Kinetic parameters of rotaxanes with axles of the same length, but different flexibilities. Note that **Rot3@2** is capable of hydrogen bonding between axle and wheel, while the other two rotaxanes are not. For readability, part of the data in Table 1 is given

with ether axles **Rot7@2**−**Rot9@2**, for which deslippage was followed in [$D_2$]tetrachloroethane. Unfortunately, we have not been able to study a rotaxane with three or even more benzene units in the axle central unit, due to insolubility in the solvents used here. Thus, we rely on the ethano bridge in axles **6** and **9**, which of course induces an element of flexibility not present in the shorter analogs. Nevertheless, the overall qualitative result of decreasing $k_\infty$ can clearly be seen and is also found for the **Rot10@2′** and **Rot11@2′** pair of rotaxanes (see below).

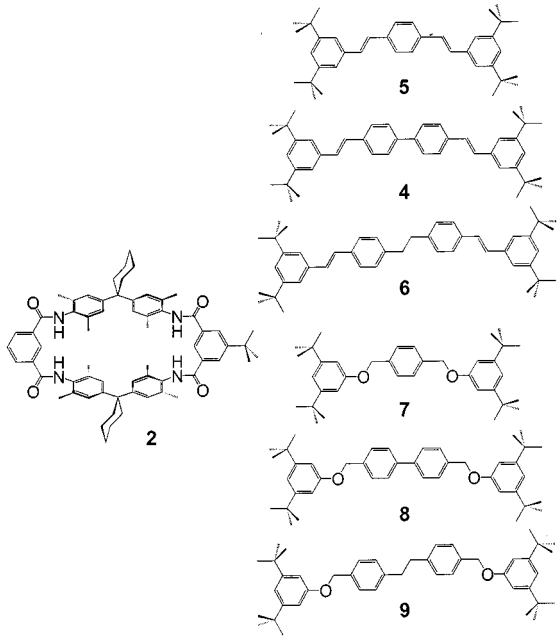


| | $E_A$ [kJ mol$^{-1}$] | $k_\infty$ [MHz] | $\Delta H^\ddagger$ [kJ mol$^{-1}$] | $\Delta S^\ddagger$ [J K$^{-1}$ mol$^{-1}$] | $t_{1/2}$ (333 K) [h] |
|---|---|---|---|---|---|
| Rot5@2 | 83 | 42 | 81 | -39 | 48 |
| Rot4@2 | 77 | 4 | 68 | -80 | 58 |
| Rot6@2 | 77 | 2 | 74 | -64 | 115 |
| Rot7@2 | 104 | 48300 | 101 | 18 | 82 |
| Rot8@2 | 98 | 12050 | 95 | 7 | 38 |
| Rot9@2 | 88 | 1530 | 85 | -10 | 8 |

Scheme 3. Kinetic parameters of rotaxanes with axles of different lengths. Note that solubility required that the series **Rot4@2**−**Rot6@2** was studied in [$D_7$]DMF, while the data for **Rot7@2**−**Rot11@2′** were collected in [$D_2$]tetrachloroethane. Direct comparison between these two series is thus not possible

More strikingly, however, the series **Rot7@2**−**Rot9@2** shows a decrease in $E_A$ (104, 98, and 88 kJ/mol, respectively) and $\Delta H^\ddagger$ (101, 95, and 85 kJ/mol) with increasing axle length. Although this effect is still not large, it is clearly beyond the experimental error limits in this series. It is also reflected in the half lives of these rotaxanes (Table 1), which decrease by a factor of 10, from 82 h for **Rot7@2** to 8 hours for **Rot9@2**. This effect is not predicted by our model and

– although we do not have a conclusive interpretation of it – clearly demonstrates that the model may serve as no more than a first approximation to a description of a rotaxane and its behavior.

Consequently, two different, but structurally closely related series of rotaxanes were found to display very different deslipping kinetics, probably due to the different solvents that had to be used in these studies, due to solubility problems. One effect might be caused by π-π interactions between axle and wheel, which should be quite different in magnitude in polar and in nonpolar solvents.

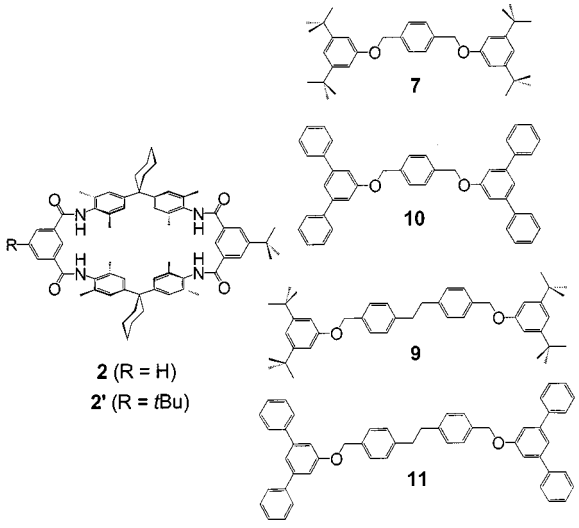


| | $E_A$ [kJ mol$^{-1}$] | $k_\infty$ [MHz] | $\Delta H^\ddagger$ [kJ mol$^{-1}$] | $\Delta S^\ddagger$ [J K$^{-1}$ mol$^{-1}$] | $t_{1/2}$ (333 K) [h] |
|---|---|---|---|---|---|
| Rot7@2 | 104 | 48300 | 101 | 18 | 82 |
| Rot10@2 | 77 | 470 | 74 | -19 | <1 |
| Rot9@2 | 88 | 1530 | 85 | -10 | 8 |
| Rot11@2 | 79 | 130 | 76 | -30 | 4 |

Scheme 4. Kinetic parameters of rotaxanes with stoppers of different sizes and shapes

### Solvent Effects

Because of solubility problems, some of the rotaxanes were examined in [$D_7$]DMF, others in [$D_2$]tetrachloroethane. The solvent was, however, kept the same within each series. All trends discussed here are derived from series of rotaxanes treated under the same conditions, and direct comparison of rotaxanes studied in different solvents has carefully been avoided. It nevertheless appeared relevant to try to establish whether there are significant solvent effects. Two rotaxanes were studied: **Rot4@2** was examined in [$D_7$]DMF and [$D_8$]THF, while the deslipping kinetics of **Rot9@2** were followed in [$D_2$]tetrachloroethane and [D]chloroform. In both cases, the effects were rather small. For **Rot9@2**, all parameters were the same within experimental error, independent of the solvent. In contrast, **Rot4@2** exhibited lower $E_A$ and $\Delta H^\ddagger$ values in [$D_8$]THF than in [$D_7$]DMF, which might be attributable to (i) hydrogen bonding between the wheel's amide protons and the solvent, which would be less pronounced in THF, and (ii) stronger π-π interactions between the two components in the more polar DMF. Nevertheless, this effect does not have any dominating effect on deslippage, although the difference between DMF and tetrachloroethane may, of course, result in much larger effects.

### Stopper Shape and Flexibility

When comparing two stoppers of different sizes, we encountered a second surprising effect (Scheme 4). The 3,5-diphenylphenyl stopper in **Rot10@2′** and **Rot11@2′**[24] has a span of ca. 11.8 Å, while the 3,5-di-*tert*-butylphenyl stopper is more than 2 Å narrower (Figure 3). In a simplified view, one would thus expect **Rot10@2′** and **Rot11@2′** to deslip more slowly than their counterparts **Rot7@2** and **Rot9@2**, respectively. Instead, the half life of **Rot10@2′** at 333 K (less than 1 hour) is more than 80 times shorter than that of **Rot7@2** (82 hours) and a similar, although less pronounced, decrease was found for the other pair.

Of course, the stoppers need not necessarily deslip with both substituents passing through the wheel at the same time; they might also follow a stepwise deslippage mechanism. Hence, one of the *tert*-butyl or phenyl groups would pass through the macrocycle first, followed by the other in the next reaction step. In this case, deslipping would involve two barriers, one of which would have to correlate to the rate-determining step. If that scenario does hold true, the total span is probably not important. Instead, a smaller effective size becomes relevant, amounting (Figure 3, a, b) to ca. 9.3 Å for the diphenyl-phenyl stopper and again being ca. 2 Å shorter for the di-*tert*-butylphenyl stopper. Consequently, the conclusion would not change. The stopper span alone thus cannot explain the results obtained from deslipping experiments.

There are, however, two effects that can probably account for the increase in deslipping rate for **Rot10@2′** and **Rot11@2′**. In terms of stopper shape, the *tert*-butyl groups represent a more spherical substituent, extending vertically from the aromatic plane by ca. 4.4 Å (Figure 3, c, d) as compared to the 3.4 Å of the phenyl substituents in axles **10** and **11**. Thus, deslippage of **Rot7@2** requires a more pronounced expansion of the wheel upon deslippage, while the rather flat diphenyl-phenyl stopper may slip through more easily. Of course, the terphenyl system in these stoppers is not perfectly planar. As in any biphenyl system, the

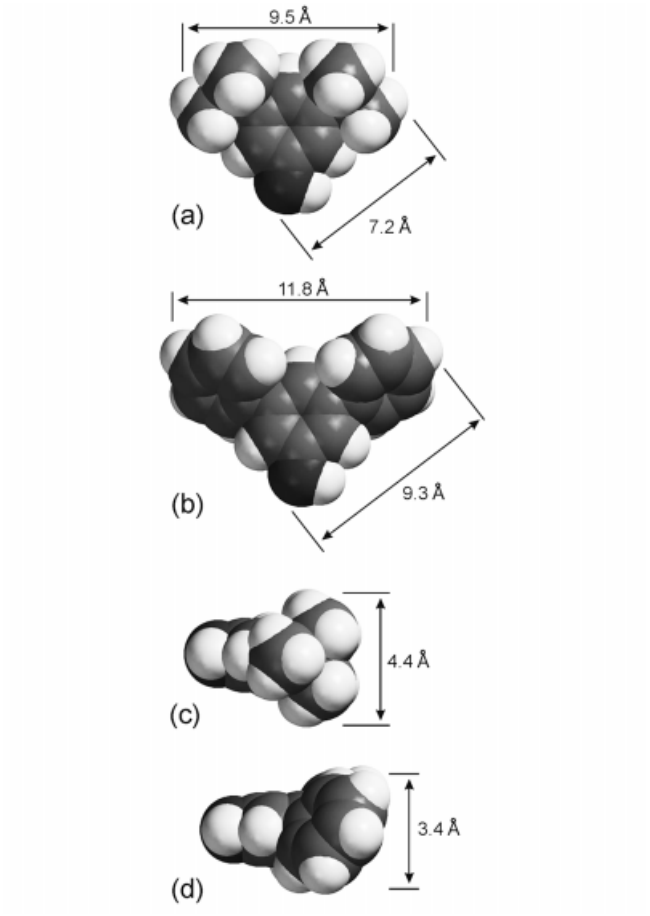


Figure 3. Top (a, b) and side (c, d) views of space-filling models of the 3,5-di-*tert*-butylphenyl and 3,5-diphenylphenyl stoppers generated with the Sybyl force field. The dimensions given for each stopper are those measured between the centers of the corresponding hydrogen atoms

two phenyl rings will be tilted somewhat out of the plane of the central ring. Nevertheless, this stopper can adapt more easily to size requirements and steric stress, because rotation of the two phenyl substituents can result in further flattening of the stopper without a large energetic demand. Rotation of the *tert*-butyl groups, on the other hand, does not produce any significant change in size and shape. This leads directly on to the second effect. Stopper flexibility might also contribute to the different kinetic behavior of **Rot7@2** and **Rot 10@2′**. If a bending motion of the phenyl rings in **Rot10@2′** were to result in a favorable geometry suitable for deslipping, the enthalpy of deslippage could even be lower than that of the more bulky, not very easily deformable, 3,5-*tert*-butyl-phenyl stopper. In other words, if the bending potential energy surface is fairly flat for a phenyl substituent, but steeper for a *tert*-butyl group, then the transition structure for deslippage of **Rot10@2′** might be energetically more favorable than that of **Rot7@2**. On the other hand, one might expect a tighter transition structure for **Rot10@2′**, resulting in higher entropic costs, since a more peculiar spatial arrangement would be required for productive deslippage. Consequently, expectation would predict lower enthalpic ($E_A$ and $\Delta H^{\ddagger}$) and higher entropic ($k_{\infty}$ and $\Delta S^{\ddagger}$) contributions to the deslipping barrier for **Rot10@2′**. Indeed, the data in Scheme 4 and Table 1 are in agreement with this interpretation. The second pair, **Rot9@2/Rot 11@2′**, for which the same effects are found, shows that our findings are not a singular case valid only for **Rot10@2′** and thus provides additional evidence.

### Tetralactam Wheel versus Sulfonamide Macrocycle

Rather than a tetralactam wheel, the rotaxanes may also feature a sulfonamide wheel, in which only one of the amides is replaced by a sulfonamide (Scheme 5), and thus only one carbonyl group is exchanged for a sulfonyl group. Practical experience has been that the sulfonamide rotaxanes deslip more quickly than those with the tetralactam macrocycle, and the assumption of a larger wheel diameter due to the longer S−C and S−N bonds has been invoked as an explanation.[16d] In our experiments, the sulfonamide rotaxanes **Rot4@12** and **Rot5@12** did indeed turn out to deslip much more rapidly than their tetralactam analogs **Rot4@2** and **Rot5@2**. The half life decreased by a factor of more than 100, from ca. 50 hours for **Rot4@2** and **Rot5@2** to less than 0.5 hours for **Rot4@12** and **Rot5@12** at 333 K. To our surprise, however, it was not the enthalpic contribution to the barrier that made the difference. That would have been to be expected, were increased bond lengths in the wheel to affect the stopper/wheel size complementarity. However, the changes in $E_A$ and $\Delta H^{\ddagger}$ are within experimental error. Much larger differences were observed in the entropic contributions. The pre-exponential factor $k_{\infty}$ increases by a factor of more than 100, and $\Delta S^{\ddagger}$ is much less negative for both sulfonamide rotaxanes as compared to their tetralactam analogs. Again, the same observation was made for two examples, confirming that it is indeed a real effect.

What chemical reason, if not the lengths of the S−C and S−N bonds, can provide the basis for an explanation of this drastic change in activation entropy? Sulfonamides differ from carbonamides in several respects. Firstly, if it has any effect on the deslipping kinetics at all, the presence of an additional oxygen atom should result in increased steric hindrance and thus a deceleration of the deslippage reaction. This is not observed and thus, most probably, the oxygen atom is not the cause of the faster decomposition of the sulfonamide rotaxanes. Secondly, the sulfur in **Rot4@12** and **Rot5@12** is more or less tetrahedral, while the carbonyl carbon in **Rot4@2** and **Rot5@2** is $sp^2$-hybridized and thus should form the center of a CCN angle rather larger than the CSN angle in **12**. Consequently, the inner diameter of the wheel might be expected to be somewhat smaller in **Rot4@12** and **Rot5@12**, again resulting in slower deslippage. Since this prediction is once more not in line with our findings, we can also rule out changes in bond angles as a reason for accelerated deslippage. Thirdly, the amide hydrogens are more acidic and so may produce stronger hydrogen bonding. However, our axles do not have any hydrogen bond acceptors (except for the π-systems of the aromatic rings, which are unlikely to play a dominant role). Thus, hydrogen bonding between axle and wheel is not possible.

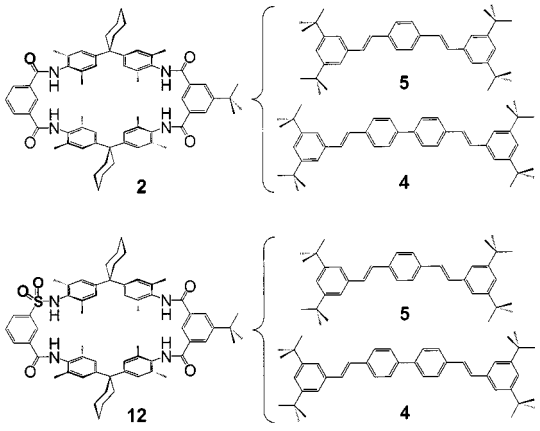


| | $E_A$ [kJ mol$^{-1}$] | $k_{co}$ [MHz] | $\Delta H^{\ddagger}$ [kJ mol$^{-1}$] | $\Delta S^{\ddagger}$ [J K$^{-1}$ mol$^{-1}$] | $t_{1/2}$ (333 K) [h] |
|---|---|---|---|---|---|
| Rot5@2 | 83 | 42 | 81 | -39 | 48 |
| Rot4@2 | 77 | 4 | 68 | -80 | 58 |
| Rot5@12 | 82 | 4940 | 75 | 0 | < 0.5 |
| Rot4@12 | 75 | 920 | 68 | -26 | < 0.5 |

Scheme 5. Kinetic parameters of rotaxanes with tetralactam wheels in comparison with those with sulfonamide wheels

Furthermore, comparison of **Rot3@2** and **Rot4@2**, studied under the same conditions, led us to the conclusion that hydrogen bonding does not play a significant role. Fourthly, rotational barriers (Scheme 6) in carbonamides have been studied intensely both experimentally[25] and theoretically[26] and are of the order of 80 kJ/mol, while those of sulfonamides have been calculated to amount to ca. 40 kJ/mol.[27] This difference is in line with the $^1$H NMR spectra of, for example, dimethyl acetamide and dimethyl methanesulfonamide. While the former shows slow exchange of the amide methyl groups, resulting in two separate signals for both, the latter gives only one signal, due to an exchange that is fast on the NMR timescale.

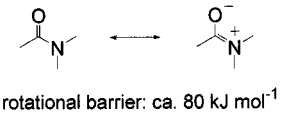


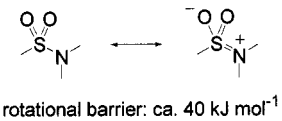


Scheme 6. Origin of the higher flexibility of the sulfonamide wheel

A lower rotational barrier for **Rot4@12** and **Rot5@12** results in an increased flexibility of the sulfonamide wheel and thus may well affect entropy. However, it affects not only the entropy of the transition structure, but also that of the rotaxane in its energetic minimum. It is thus not clear a priori that increased flexibility should necessarily result in an increased entropy of activation. Indeed, the examples of different stoppers discussed above represent the opposite case, in which entropic disadvantages are compensated for by a beneficial enthalpic situation. Seemingly, this is not feasible in the case of **Rot4@12** and **Rot5@12**, and a favorable entropic situation is found, with an almost unchanged enthalpic contribution to the barrier.

### Intracycle Hydrogen Bonding and its Effect on the Deslipping Rate

The largest effect, however, is observed for rotaxanes that again differ in only a minor structural variation. The wheel in **Rot3@2** bears two isophthalic amide building blocks, while in **Rot3@13** one of these is exchanged for a 2,6-pyridinedicarboxylic acid diamide subunit (Scheme 7). Thus, these two wheels differ only in the replacement of a C−H group for an isoelectronic nitrogen atom. Despite this small structural change, the half lives of the two compounds differ by more than a factor of $10^4$. The half life of ca. 60 hours at 333 K for **Rot3@2** increases to a calculated value of more than 1 million hours for **Rot3@13**, which reflects the fact that it is possible to follow the deslipping kinetics of **Rot3@2** in a temperature range of around 300 to 380 K, while **Rot3@13** requires temperatures between 390 and 450 K for a reasonable, but still much longer, timeframe. This huge difference is due to a much higher barrier $E_A$, which is of the order of 130 kJ/mol for **Rot3@13** while amounting to only ca. 80 kJ/mol for **Rot3@2**. In contrast, the difference in entropy is rather small. The same trends can be seen in the Eyring parameters. For rotaxane **Rot3@14**, with two 2,6-pyridinedicarboxylic acid diamide blocks, the changes are even more pronounced; no deslippage was observed at all, although the sample of **Rot3@14** was kept at 423 K for a prolonged period.

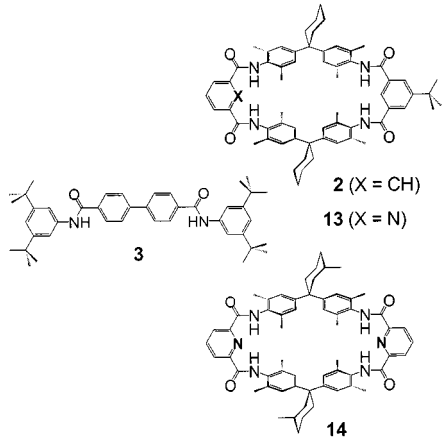


| | $E_A$ [kJ mol$^{-1}$] | $k_{co}$ [MHz] | $\Delta H^{\ddagger}$ [kJ mol$^{-1}$] | $\Delta S^{\ddagger}$ [J K$^{-1}$ mol$^{-1}$] | $t_{1/2}$ (333 K) [h] |
|---|---|---|---|---|---|
| Rot3@2 | 81 | 16 | 78 | -49 | 61 |
| Rot3@13 | 134 | 50 | 130 | -40 | > $10^6$ |
| Rot3@14 | no deslipping observed | | | | |

Scheme 7. Kinetic parameters of rotaxanes with isophthalic amide and pyridinedicarboxylic acid diamide building blocks in the wheels. Note that wheel **14** has one additional methyl group attached to each of the cyclohexyl rings. Without these methyl groups the macrocycle is insoluble and does not permit rotaxane synthesis

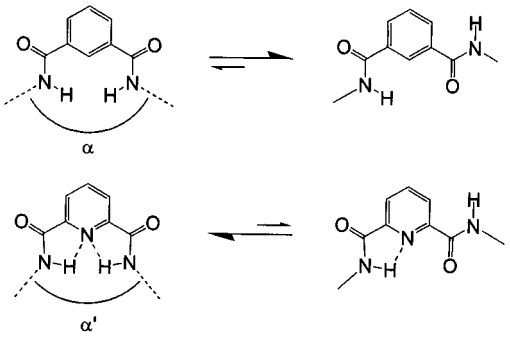

Scheme 8. Conformational preferences and hydrogen bonding patterns found for the pyridino wheel, compared with those of the tetralactam macrocycle with isophthalic amide subunits

The explanation for this large effect certainly does not involve the hydrogen atom missing in the pyridine case. A hydrogen atom occupies more space inside the wheel than the nitrogen lone pair does, and so deslippage should be faster with the pyridine building block. However, a search for an explanation uncovers several literature reports on the extraordinary properties of the 2,6-pyridinedicarboxylic acid diamide building block. From X-ray structures of benzylamide catenanes,[28] furano catenanes,[29] and open chain analogs,[31a] it is known to form hydrogen bonds between the amide protons and the central pyridine nitrogen or furane oxygen (Scheme 8). This hydrogen bonding pattern has been reported to cause slower circumrotation in benzylamide catenanes[30] and to change the angle α (Scheme 8) from 120° to an α′ of ca. 90−100° in open chain analogs.[31] This difference in α is probably smaller in our macrocyclic wheels, because of the rather rigid structure of the macrocycle. Nevertheless, it may well alter the deslipping rate significantly, thanks to a smaller wheel diameter and the corresponding increase in the deslipping barrier.

A second effect might also contribute. The hydrogen bonding pattern of the 2,6-pyridinedicarboxylic acid diamide subunit also shifts the conformational equilibrium of the two amides towards the *in*/*in* conformation, with the two amide protons pointing towards the center of the macrocycle as shown in Scheme 8.[32] As seen in X-ray structures of rotaxanes and catenanes of the amide type,[23] isophthalic amides such as in **2** often adopt an *in*/*out* conformation, which is further disfavored in **13** and **14** by repulsion between the lone pairs situated at the carbonyl oxygens and the pyridine nitrogen atom. With a more or less fixed conformation with both amide protons inside the wheel, the space available for the passage of the stopper through the wheel becomes even smaller. We believe that these two effects explain the large difference in deslipping rates.

## Conclusions

This study shows that our simplified starting hypothesis is only valid as a first and rather rough approximation. To regard a rotaxane merely as a slender stick threaded through a wheel and capped by two bulky end groups is too simplified a view for detailed analysis of the deslipping kinetics. Not unexpectedly, rotaxanes, as rather complex systems, display complicated behavior. This result has some conceptual implications for analysis of the size complementarity of stoppers and wheels as used previously to determine the ranking of dendritic stoppers by Vögtle et al.[16a] The authors cautiously speak of the "effective size" of the stoppering dendrons. As corroborated by our finding that seemingly larger stoppers can deslip more quickly due to their shape and flexibility, similar effects might occur with dendritic stopper groups. A large dendron might still allow faster deslippage, if it is flexible enough to slip through the wheel by means of a multi-step process, one branch after the other. Thus, careful analysis of the kinetic parameters is suggested in deslipping experiments, if conclusions are drawn with respect to the size complementarity.

This highlights the major argument, of why the simplified view of a rotaxane presented at the start is only a first order approximation. Even if structural changes do not change the static properties such as ring size much, they may profoundly alter the dynamic behavior of the rotaxane. Indeed, with the sulfonamide wheels, the terphenyl stoppers, and the hydrogen bonding within the pyridinedicarboxylic acid diamide building blocks, effects that are dynamic in nature have been observed. Clearly, a purely static model for deslipping cannot provide a satisfying explanation if dynamics play such an important role.

Another interesting observation is the magnitude of some of the effects observed. In particular, the introduction of a 2,6-pyridinedicarboxylic acid diamide building block into the wheel produces enormous effects. This in turn implies that deslipping − when completely understood and carefully interpreted − may be developed into a sensitive tool for the examination of steric parameters.

Our study identifies several features that have an important influence on rotaxane deslipping kinetics, all of which need more in-depth investigation in order to provide more profound understanding of the intramolecular mobility and the dynamic processes associated with the deslipping reaction. These are: (i) the size complementarity of stoppers and wheel, (ii) the shape and flexibility of the rotaxanes' components, (iii) the effect of weak intramolecular forces such as hydrogen bonds that, for example, stabilize certain conformations, and (iv) potentially the solvent and the effects caused by its reorganization. As an initial survey, the knowledge gained about these parameters is a great help in defining the next steps in this project, which will be reported in due course.

## Experimental Section

**Kinetic Studies:** For each of the rotaxanes, the rate constants of the deslipping reaction were measured at several different temperatures in $^1$H NMR experiments. In preliminary experiments, the temperature range was chosen so that deslipping occurred with a half life of between one and ca. 400 hours. The NMR samples were kept in an oil bath at constant temperature. When the half life was found

to be sufficiently short at temperatures accessible with the NMR instrument's heater, the samples were transferred to the NMR spectrometer. In each experiment, deslipping was followed until at least 75% of the rotaxane had been consumed. For evaluation of the data, integrals of several signals were averaged wherever possible, in order to reduce experimental error. However, some of the rotaxanes produced NMR spectra in which decreasing and increasing signals overlapped to such an extent that only one or two of the signals could be evaluated safely. The estimated experimental error range is ±4 kJ/mol for $E_A$ and $\Delta H^{\ddagger}$. Because of the logarithmic nature of the plots, the errors in $k_{\infty}$ and $\Delta S^{\ddagger}$ are somewhat larger and we estimate them to be ±30% for $k_{\infty}$ and $\Delta S^{\ddagger}$. The Arrhenius activation parameters were derived from a plot of ln $k$ against $1/T$, while ln ($k/T$) was plotted against $1/T$ in order to determine $\Delta G^{\ddagger}$, $\Delta H^{\ddagger}$, and $\Delta S^{\ddagger}$ by the Eyring equation. Close inspection of those signals increasing over time confirmed that they corresponded to the intact free components and thus ruled out decomposition of the axle or wheel rather than deslipping as the reason for rotaxane degradation. Unfortunately, solubility problems forced us to measure some of the rotaxanes in [$D_7$]DMF and the series of ether rotaxanes in [$D_2$]tetrachloroethane. These two series thus cannot be compared directly, but trends emerging within each of them can of course be analyzed. Finally, for correlation with the activation parameters, the axle lengths and the stopper size were determined by molecular modeling with the Sybyl force field as implemented in the Spartan program package[33] according to the definition given in Figures 1 and 3.

**Synthesis of Rotaxanes:** In terms of their syntheses, the rotaxanes selected for this study fall into three different groups.

(i) The first series bears axles that are purely hydrocarbon in nature (**Rot1@2**, **Rot4@2**−**Rot6@2**, **Rot4@12**, **Rot5@12**). This type of axle reduces the possible complications arising from noncovalent forces between axle and wheel. As the axles were deliberately selected to be rigid, the aromatic ring systems could not be avoided. Synthesis was achieved by melting mixtures of axle and wheel at 350 °C for a short time interval and separating the rotaxane from the remaining reactants.[19] The precursors, 3,5-diphenylphenol,[34] axles[35] **1**, **4**, **5**, and **6**, and wheels **2**,[36] **12**,[37] **13**,[32] and **14**,[32] were prepared according to well established literature procedures. Macrocycle **14** has a methyl group attached to each of the cyclohexyl rings to improve solubility. Attempted rotaxane synthesis using the same wheel but without these methyl groups was not successful.[38]

(ii) **Rot7@2**−**Rot11@2′** are rotaxanes with ether groups in the axles. Synthesis could easily be accomplished using a recently published anion template effect.[39] With a few exceptions (see below), the synthetic precursors for the series of ether rotaxanes were commercially available and were used without further purification.

(iii) The third series (**Rot3@2**, **Rot3@13**, **Rot3@14**) features amide groups in the axle that are capable of forming three hydrogen bonds with the wheel. **Rot3@2** was prepared by melting synthesis as described above; the other two were synthesized by a template synthesis, in which the semi-axle was fitted with the second stopper while held within the wheel by hydrogen bonds.[40]

Characterization of the rotaxanes was sometimes obstructed by deslipping being quite fast even at room temperature, with a proportion of the rotaxane degrading during column chromatography. Elemental analyses are consequently not always within the usually accepted range and are further complicated by varying amounts of solvents that could not entirely be removed from the samples. We therefore base the characterization of the target compounds mainly on $^1$H and $^{13}$C NMR experiments, for which signal assignment was accomplished by DEPT and CH-COSY measurements. All NMR experiments were performed on 250, 400, and 500 MHz Bruker instruments; the solvent signal was used for internal calibration. NMR spectra of those rotaxanes that dethread quickly of course also contain small signals from the free components. In the measurements of deslipping over time, the data were corrected for these initial contributions of the free components. Furthermore, all rotaxanes gave clean FAB (Kratos Concept 1 H) or MALDI (Micromass MALDI-TofSpec-E) mass spectra that − apart from signals originating from the matrices (*m*-nitrobenzyl alcohol and dihydroxybenzoic acid, respectively) − contained only prominent peaks for the rotaxane, free axle, and free wheel, a pattern that is typical for these rotaxanes. Under the same conditions, mixtures of the free components do not give signals at the *m*/*z* ratio of the rotaxanes, indicating that these signals, when indeed observed, are due to the intact rotaxane rather than any proton-bridged complex without a mechanical bond. The isotope patterns agree well with those calculated on the basis of natural abundances.

**General Procedure for the Melting Synthesis:** Equimolar amounts of the corresponding macrocycle and axle were thoroughly mixed under argon and the mixture was melted with a heat gun at about 350 °C. After the reaction mixture had been chilled in cold water, the residue was dissolved in $CH_2Cl_2$/MeOH 5:1 and subjected to column chromatography on silica gel with dichloromethane/ethyl acetate ($CH_2Cl_2$/EtOAc) mixtures.

***Axle 3*: *N,N′*-Bis(3,5-di-*tert*-butylphenyl)-4,4′-biphenyldicarboxylic Acid Diamide:**[19i] Yield: 53%; m.p. > 300 °C. − $^1$H NMR (250 MHz, [$D_7$]DMF) δ (ppm) = 1.34 [s, 36 H, C($CH_3$)$_3$], 7.27 (s, 2 H, Ar-H), 7.88 (s, 4 H, Ar-H), 7.98 (*AA′*BB′, $^3J$ = 8.3 Hz, 4 H, Ar-H), 8.23 (AA′*BB′*, $^3J$ = 8.3 Hz, 4 H, Ar-H), 10.30 (s, 2 H, NH). − $^{13}$C NMR (62.9 MHz, $CDCl_3$/$CD_3OD$) δ (ppm) = 31.65 ($CH_3$), 35.39 (Cq), 115.50, 118.25, 127.75, 129.00 (CH), 135.63, 143.15, 151.70 (Cq), 165.80 (CO). − FAB-MS: *m*/*z* = 617.4 [M + H$^+$].

***Axle 6*: *E,E*-4,4′-Bis(3,5-di(*tert*-butyl)phenylethenyl]-1,1′-bibenzyl:**[35] Yield: 52%; m.p. 177−180 °C. − $^1$H NMR (250 MHz, $CDCl_3$) δ (ppm) = 1.37 [s, 36 H, C($CH_3$)$_3$], 2.95 (s, 4 H, $CH_2$), 7.07 (*A*B, $^3J$ = 16.6 Hz, 2 H, vinyl-H), 7.17 (A*B*, $^3J$ = 16.6 Hz, 2 H, vinyl-H), 7.18 (d, $^3J$ = 8 Hz, 4 H, Ar-H), 7.37 (m, 6 H, Ar-H), 7.47 (d, $^3J$ = 8 Hz, 4 H, Ar-H). − $^{13}$C NMR (100.6 MHz, $CDCl_3$) δ (ppm) = 31.56 ($CH_3$), 34.95 ($CH_2$), 37.70 (Cq), 120.86, 122.04, 126.52, 127.94, 128.88, 129.16 (CH), 135.50, 136.73, 141.12, 151.07 (Cq). − FAB-MS: *m*/*z* = 610.3 [M$^{+\cdot}$].

***Rot1@2*: [2]{(*E*,E)-4,4′-Bis[3,5-di(*tert*-butyl)phenylethyl]-1,1′-biphenyl}-{11′-*tert*-butyl-5′,17′,23′,35′,38′,40′,43′,45′-octamethyldispiro[cyclohexane-1,2′-7′,15′,25′,33′-tetraazaheptacyclo-[32.2.2.2$^{3'.6'}$.2$^{16'.19'}$.2$^{21'.24'}$.1$^{9'.13'}$.1$^{27'.31'}$]hexatetraconta-3′,5′,9′,11′,13′(44′),16′,18′,21′,23′,27′,29′,31′(39′),34′,36′,37′,40′,42′,45′-octadecaene-20′,1′′-cyclohexane]-8′,14′,26′,32′-tetrone}rotaxane:** $R_f$ = 0.55 ($CH_2Cl_2$/EtOAc = 20:1); yield: 3%; m.p. 136−140 °C. − $^1$H NMR (500 MHz, [$D_8$]THF) δ (ppm) = 1.29 [s, 36 H, C($CH_3$)$_3$], 1.36 [s, 9 H, C($CH_3$)$_3$], 1.56 (br. s, 4 H, $CH_2$), 1.71 (br. s, 8 H, $CH_2$), 1.96 (s, 12 H, Ar-$CH_3$), 1.97 (s, 12 H, Ar-$CH_3$), 2.43 (br. s, 8 H, $CH_2$), 2.67 (br. s, 8 H, $CH_2$), 6.71 (s, 8 H, Ar-H), 7.02 (d, $^4J$ = 1.7 Hz, 4 H, Ar-H), 7.14 (s, 4 H, Ar-H), 7.16 (s, 4 H, Ar-H) 7.25 (t, $^4J$ = 1.7 Hz, 2 H, Ar-H), 7.51 (t, $^3J$ = 7.7 Hz, 1 H, Ar-H), 7.63 (t, $^4J$ = 1.6 Hz, 1 H, Ar-H), 7.66 (s, 2 H, CONH), 7.82 (s, 2 H, CONH), 7.84 (t, $^4J$ = 1.6 Hz, 1 H, Ar-H), 7.93 (dd, $^3J$ = 7.7, $^4J$ = 1.6 Hz, 2 H, Ar-H), 8.05 (d, $^4J$ = 1.6 Hz, 2 H, Ar-H). − $^{13}$C NMR (125 MHz, [$D_8$]THF) δ (ppm) = 19.6, 19.7, 31.8, 32.2 ($CH_3$), 24.3, 27.8, 36.9, 38.9, 39.6 ($CH_2$), 120.9, 123.5, 125.3, 127.3, 127.4, 127.5,

128.2, 128.5, 129.7, 130.0, 131.3 (CH), 35.7, 46.4, 134.0, 134.1, 135.5, 135.8, 136.8, 137.1, 138.6, 142.0, 142.2, 148.6, 148.7, 151.6, 153.6 (Cq), 166.0, 166.1 (CO). − FAB-MS: *m/z* (%) = 1574.9 (50) [M + H$^+$].

***Rot3@2:*** **[2]{*N,N*′-Bis[3,5-di(*tert*-butyl)phenyl]-1,1′-biphenyl-4,4′-dicarboxamide}-{11′-*tert*-butyl-5′,17′,23′,35′,38′,40′,43′,45′-octamethyldispiro[cyclohexane-1,2′-7′,15′,25′,33′-tetraazaheptacyclo[32.2.2.2$^{3'.6'}$.2$^{16'.19'}$.2$^{21'.24'}$.1$^{9'.13'}$.1$^{27'.31'}$]hexatetraconta-3′,5′,9′,11′,13′(44′),16′,18′,21′,23′,27′,29′,31′(39′),34′,36′,37′,40′,42′,45′-octadecaene-20′,1′′-cyclohexane]-8′,14′,26′,32′-tetrone}rotaxane:** $R_f$ = 0.45 ($CH_2Cl_2$/EtOAc = 30:1); yield: 7%; m.p. > 300 °C. − $^1$H NMR (500 MHz, [D$_7$]DMF) δ (ppm) = 1.29 [s, 36 H, C(CH$_3$)$_3$], 1.39 [s, 9 H, C(CH$_3$)$_3$], 1.50 (br. s, 4 H, CH$_2$), 1.60 (br. s, 8 H, CH$_2$), 2.01 (s, 24 H, CH$_3$), 2.45 (br. s, 8 H, CH$_2$), 7.09 (d, $^3J$ = 7.5 Hz, 4 H, Ar-H), 7.25 (s, 8 H, Ar-H), 7.27 (s, 2 H, Ar-H), 7.55 (d, $^3J$ = 7.5 Hz, 4 H, Ar-H), 7.67 (s, 4 H, Ar-H), 7.69 (t, $^3J$ = 7.4 Hz, 1 H, Ar-H), 8.08 (d, $^3J$ = 7.4 Hz, 2 H, Ar-H), 8.14 (s, 2 H, Ar-H), 8.30 (s, 1 H, Ar-H), 8.45 (s, 1 H, Ar-H), 9.00 (s, 2 H, CONH), 9.02 (s, 2 H, CONH), 9.72 (s, 2 H, CONH). − $^{13}$C NMR (125 MHz, [D$_7$]DMF) δ (ppm) = 19.02, 31.38, 31.61, 23.62, 26.89, 25.09, 35.39, 35.50, 35.72, 45.73, 115.44, 118.70, 126.35, 126.85, 124.82, 127.20, 128.06, 128.63, 128.82, 129.81, 131.18, 133.50, 133.56, 134.87, 135.53, 135.56, 135.76, 135.91, 139.46, 142.72, 147.94, 151.67, 153.01, 166.01, 166.25, 166.67. − FAB-MS: *m/z* (%) = 1578.1 (70) [M + H$^+$]. − $C_{106}H_{124}N_6O_6$·2H$_2$O (1614.21): calcd. C 78.87, H 7.99, N 5.21; found C 78.96, H 8.59, N 5.18.

***Rot4@2:*** **[2]{(*E*,E)-4,4′-Bis[3,5-di(*tert*-butyl)phenylethenyl]-1,1′-biphenyl}-{11′-*tert*-butyl-5′,17′,23′,35′,38′,40′,43′,45′-octamethyldispiro[cyclohexane-1,2′-7′,15′,25′,33′-tetraazaheptacyclo[32.2.2.2$^{3'.6'}$.2$^{16'.19'}$.2$^{21'.24'}$.1$^{9'.13'}$.1$^{27'.31'}$]hexatetraconta-3′,5′,9′,11′,13′(44′),16′,18′,21′,23′,27′,29′,31′(39′),34′,36′,37′,40′,42′,45′-octadecaene-20′,1′′-cyclohexane]-8′,14′,26′,32′-tetrone}rotaxane:** $R_f$ = 0.40 ($CH_2Cl_2$/EtOAc = 30:1); yield: 3%; m.p. 208 °C. − $^1$H NMR (400 MHz, [D$_8$]THF) δ (ppm) = 1.33 [s, 36 H, C(CH$_3$)$_3$], 1.37 [s, 9 H, C(CH$_3$)$_3$], 1.51 (br. s, 4 H, CH$_2$), 1.71(br. s, 8 H, CH$_2$), 1.97 (s, 12 H, CH$_3$), 1.99 (s, 12 H, CH$_3$), 2.47 (br. s, 8 H, CH$_2$), 6.90 (d, $^3J$ = 16.3 Hz, 2 H, vinyl-H), 6.97 (d, $^3J$ = 8.5 Hz, 4 H, Ar-H), 7.04 (d, $^3J$ = 8.5 Hz, 4 H, Ar-H), 7.05 (d, $^3J$ = 16.3 Hz, 2 H, vinyl-H), 7.15 (s, 8 H, Ar-H), 7.35 (t, $^4J$ = 1.7 Hz, 2 H, Ar-H), 7.37 (d, $^4J$ = 1.7 Hz, 4 H, Ar-H), 7.51 (t, $^3J$ = 7.6, 1 H, Ar-H), 7.75 (t, $^4J$ = 1.6 Hz, 1 H, Ar-H), 7.85 (s, 2 H, CONH), 7.93 (d, $^4J$ = 1.6 Hz, 2 H, Ar-H), 7.95 (d, $^3J$ = 7.6, 2 H, Ar-H), 8.04 (d, $^4J$ = 1.6 Hz, 1 H, Ar-H), 2NH covered by signal at 7.95. − $^{13}$C NMR (125 MHz, [D$_8$]THF) δ (ppm) = 16.62, 16.81, 16.85, 29.13, 29.42, 34.30, 21.66, 22.89, 25.09, 33.07, 43.93, 119.36, 120.17, 122.66, 124.76, 124.82, 125.25, 125.53, 125.75, 127.16, 127.78, 128.36, 131.34, 131.41, 133.43, 134.12, 134.38, 134.97, 135.36, 136.96, 145.99, 149.22, 150.75, 163.38, 163.38, 163.53. − FAB-MS: *m/z* (%) = 1544.0 (52) [M + H$^+$]. − $C_{108}H_{126}N_4O_4$·2H$_2$O (1579.71): calcd. C 82.09, H 8.29, N 3.55; found C 82.19, H 8.49, N 2.90.

***Rot5@2:*** **[2]{(*E,E*)-4,4′-Bis[3,5-di(*tert*-butyl)phenylethenyl]benzene}-{11′-*tert*-butyl-5′,17′,23′,35′,38′,40′,43′,45′-octamethyldispiro[cyclohexane-1,2′-7′,15′,25′,33′-tetraazaheptacyclo[32.2.2.2$^{3'.6'}$.2$^{16'.19'}$.2$^{21'.24'}$.1$^{9'.13'}$.1$^{27'.31'}$]hexatetraconta-3′,5′,9′,11′,13′(44′),16′,18′,21′,23′,27′,29′,31′(39′),34′,36′,37′,40′,42′,45′-octadecaene-20′,1′′-cyclohexane]-8′,14′,26′,32′-tetrone}rotaxane:** $R_f$ = 0.56 ($CH_2Cl_2$/EtOAc = 20:1); yield: 13%; m.p. 215−218 °C. − $^1$H NMR (500 MHz, [D$_8$]THF) δ (ppm) = 1.29 [s, 36 H, C(CH$_3$)$_3$], 1.37 [s, 9 H, C(CH$_3$)$_3$], 1.58 (br. s, 4 H, CH$_2$), 1.72 (br. s, 8 H, CH$_2$), 1.97 (s, 12 H, Ar-CH$_3$), 1.99 (s, 12 H, Ar-CH$_3$), 2.41 (br. s, 8 H, CH$_2$), 6.64 (s, 4 H, Ar-H), 6.75 (d, $^3J$ = 16.3 Hz, 2 H, vinyl-H), 6.91 (d, $^3J$ = 16.3 Hz, 2 H, vinyl-H), 7.09 (s, 4 H, Ar-H), 7.10 (s, 4 H, Ar-H), 7.29 (d, $^4J$ = 1.7 Hz, 4 H, Ar-H), 7.30 (t, $^4J$ = 1.7 Hz, 2 H, Ar-H), 7.52 (t, $^3J$ = 7.7 Hz, 1 H, Ar-H), 7.85 (t, $^4J$ = 1.5 Hz, 1 H, Ar-H), 7.90 (s, 2 H, CONH), 7.96 (dd, $^3J$ = 7.7, $^4J$ = 1.6 Hz, 2 H, Ar-H), 8.01 (s, 2 H, CONH), 8.06 (d, $^4J$ = 1.5 Hz, 2 H, Ar-H), 8.07 (d, $^4J$ = 1.6 Hz, 1 H, Ar-H). − $^{13}$C NMR (125 MHz, [D$_8$]THF) δ (ppm) = 19.0, 19.1, 23.9, 27.3, 31.4, 31.6, 35.3, 35.6, 36.7, 46.2, 121.6, 122.3, 124.9, 127.1, 127.2, 127.6, 127.8, 128.4, 129.4, 129.7, 130.4, 133.5, 133.6, 135.8, 136.5, 136.7, 137.0, 137.7, 148.4, 151.4, 153.0, 165.6, 165.8. − FAB-MS: *m/z* (%) = 1467.7 (78) [M + H$^+$].

***Rot6@2:*** **[2]{(*E,E*)-4,4′-Bis[3,5-di(*tert*-butyl)phenylethenyl]-1,1′-bibenzyl}-{11′-*tert*-butyl-5′,17′,23′,35′, 38′,40′,43′,45′-octamethyldispiro[cyclohexane-1,2′-7′,15′,25′,33′-tetraazaheptacyclo-[32.2.2.2$^{3'.6'}$.2$^{16'.19'}$.2$^{21'.24'}$.1$^{9'.13'}$.1$^{27'.31'}$]hexatetraconta-3′,5′,9′,11′,13′(44′),16′,18′,21′,23′,27′,29′,31′(39′),34′,36′,37′,40′,42′,45′-octadecaene-20′,1′′-cyclohexane]-8′,14′,26′,32′-tetrone}rotaxane:** $R_f$ = 0.60 ($CH_2Cl_2$/EtOAc = 20:1); yield: 8%; m.p. 187−190 °C. − $^1$H NMR (500 MHz, [D$_8$]THF) δ (ppm) = 1.31 [s, 36 H, C(CH$_3$)$_3$], 1.37 [s, 9 H, C(CH$_3$)$_3$], 1.57 (br. s, 4 H, CH$_2$), 1.71 (br. s, 8 H, CH$_2$), 1.97 (s, 12 H, Ar-CH$_3$), 1.99 (s, 12 H, Ar-CH$_3$), 2.42 (br. s, 8 H, CH$_2$), 2.63 (s, 4 H, CH$_2$), 6.78 (d, $^3J$ = 16.3 Hz, 2 H, vinyl-H), 6.79 (d, $^3J$ = 8.1 Hz, 4 H, Ar-H), 6.91 (d, $^3J$ = 8.1 Hz, 4 H, Ar-H), 7.03 (d, $^3J$ = 16.3 Hz, 2 H, vinyl-H), 7.09 (s, 4 H, Ar-H), 7.10 (s, 4 H, Ar-H), 7.31 (s, 2 H, Aryl-H), 7.33 (s, 4 H, Aryl-H), 7.50 (t, $^3J$ = 7.7 Hz, 1 H, Ar-H), 7.88 (t, $^4J$ = 1.4 Hz, 1 H, Ar-H), 7.93 (s, 2 H, CONH), 7.96 (dd, $^3J$ = 7.7, $^4J$ = 1.4 Hz, 2 H, Ar-H), 8.05 (s, 2 H, CONH), 8.09 (s, 2 H, Ar-H), 8.10 (s, 1 H, Ar-H). − $^{13}$C NMR (125 MHz, [D$_8$]THF) δ (ppm) = 19.5, 19.6, 24.4, 27.8, 31.9, 32.2, 35.8, 37.0, 38.5, 46.6, 122.0, 122.6, 125.5, 127.5, 128.3, 128.5, 128.9, 129.7, 129.9, 131.1, 134.0, 134.1, 136.1, 136.5, 136.8, 137.1, 138.3, 141.9, 148.7, 151.9, 153.5, 166.1, 166.2. − MALDI-TOF-MS: *m/z* (%) = 1572.40 (95) [M + H$^+$].

***Rot4@12:*** **[2]{(*E,E*)-4,4′-Bis[3,5-di(*tert*-butyl)phenylethenyl]-1,1′-biphenyl}-{11′-*tert*-butyl-5′,17′,23′,35′,38′,40′,43′,45′-octamethyldispiro[cyclohexane-1,2′-26-thia-7′,15′,25′,33′-tetraazaheptacyclo[32.2.2.2$^{3'.6'}$.2$^{16'.19'}$.2$^{21'.24'}$.1$^{9'.13'}$.1$^{27'.31'}$]hexatetraconta-3′,5′,9′,11′,13′(44′),16′,18′,21′,23′,27′,29′,31′(39′),34′,36′,37′,40′,42′,45′-octadecaene-20′,1′′-cyclohexane]-8′,14′,32′-trione-26′,26′-dioxide} rotaxane:** $R_f$ = 0.77 ($CH_2Cl_2$/EtOAc = 20:1); yield: 4% (contains ca. 30% deslipping products). − $^1$H NMR (500 MHz, [D$_8$]THF) δ (ppm) = 1.37 [s, 36 H, C(CH$_3$)$_3$], 1.40 [s, 9 H, C(CH$_3$)$_3$], 1.50−1.55 (br. s, 8 H, CH$_2$), 1.66 (br. s, 4 H, CH$_2$), 1.99 (s, 6 H, Ar-CH$_3$), 2.02 (s, 6 H, Ar-CH$_3$), 2.06 (s, 6 H, Ar-CH$_3$), 2.07 (s, 6 H, Ar-CH$_3$), 2.37 (br. s, 8 H, CH$_2$), 6.89 (d, $^3J$ = 16.7 Hz, 2 H, vinyl-H), 7.01 (d, $^3J$ = 8.3 Hz, 4 H, Ar-H), 7.08 (s, 2 H, Ar-H), 7.09 (d, $^3J$ = 8.4 Hz, 4 H, Ar-H), 7.13 (s, 2 H, Ar-H), 7.19 (d, $^3J$ = 16.7 Hz, 2 H, Ar-H), 7.20 (s, 1 H, Ar-H), 7.31 (s, 2 H, Ar-H), 7.40 (t, $^4J$ = 1.8 Hz, 2 H, Ar-H), 7.48 (d, $^4J$ = 1.8 Hz, 2 H, Ar-H), 7.85 (t, $^3J$ = 7.9 Hz, 1 H, Ar-H), 8.07 (s, 1 H, Ar-H), 8.09 (s, 1 H, Ar-H), 8.20 (s, 1 H, Ar-H), 8.24 (s, 1 H, Ar-H), 8.32 (d, $^3J$ = 7.9 Hz, 2 H, Ar-H), 8.69 (s, 1 H, CONH), 8.94 (s, 1 H, CONH), 9.04 (s, 1 H, CONH), 9.12 (s, 1 H, SO$_2$NH); due to rapid deslipping (half-life time at room temperature: < 2 hours), no $^{13}$C NMR was recorded. − FAB-MS: *m/z* (%) = 1579.9 (30) [M + H$^+$].

***Rot5@12:*** **[2]{(*E,E*)-4,4′-Bis[3,5-di(*tert*-butyl)phenylethenyl]benzene}-{11′-*tert*-butyl-5′,17′,23′,35′,38′,40′,43′,45′-octamethyldispiro[cyclohexane-1,2′-26-thia-7′,15′,25′,33′-tetraazaheptacyclo-[32.2.2.2$^{3'.6'}$.2$^{16'.19'}$.2$^{21'.24'}$.1$^{9'.13'}$.1$^{27'.31'}$]hexatetraconta-3′,5′,9′,11′,13′(44′),16′,18′,21′,23′,27′,29′,31′(39′),34′,36′,37′,40′,42′,45′octadecaene-20′,1′′-cyclohexane]-8′,14′,32′-trione-26′,26′-**

**dioxide}rotaxane:** $R_f$ = 0.50 ($CH_2Cl_2$/EtOAc = 20:1); yield: 5% (contains ca. 20% deslipping products), $^1$H NMR (500 MHz, [D$_8$]THF) δ (ppm) = 1.35 [s, 36 H, C(CH$_3$)$_3$], 1.36 [s, 9 H, C(CH$_3$)$_3$], 1.46−1.59 (br. s, 8 H, CH$_2$), 1.61−1.70 (br. s, 4 H, CH$_2$), 1.90 (s, 6 H, Ar-CH$_3$), 2.07 (s, 6 H, Ar-CH$_3$), 2.09 (s, 6 H, Ar-CH$_3$), 2.11 (s, 6 H, Ar-CH$_3$), 2.37−2.46 (br. s, 8 H, CH$_2$), 6.51 (s, 4 H, Ar-H), 6.53 (d, $^3J$ = 17.5 Hz, 2 H, vinyl-H), 7.04 (d, $^3J$ = 17.5 Hz, 2 H, vinyl-H), 7.08 (s, 2 H, Ar-H), 7.22 (s, 2 H, Ar-H), 7.27 (s, 2 H, Ar-H), 7.30 (s, 2 H, Ar-H), 7.37 (t, $^4J$ = 1.7 Hz, 2 H, Ar-H), 7.42 (d, $^4J$ = 1.7 Hz, 4 H, Ar-H), 7.81 (t, $^3J$ = 7.8 Hz, 1 H, Ar-H), 8.09 (t, $^4J$ = 1.7 Hz, 2 H, Ar-H), 8.14 (t, $^4J$ = 1.7 Hz, 1 H, Ar-H), 8.33 (d, $^3J$ = 7.8 Hz, 1 H, Ar-H), 8.42 (d, $^3J$ = 7.8 Hz, 1 H, Ar-H), 8.43 (s, 1 H, Ar-H), 8.74 (s, 1 H, CONH), 8.99 (s, 1 H, CONH), 9.19 (s, 1 H, CONH), 9.28 (s, 1 H, SO$_2$NH); due to rapid deslipping (half-life at room temperature: < 2 hours), no $^{13}$C NMR was recorded. − FAB-MS: *m*/*z* (%) = 1503.7 (30) [M + H$^+$].

**General Procedure for the Synthesis of Ether Rotaxanes:** The wheel was stirred in dichloromethane, together with 1 equiv. of the axle's dibromide central unit, 2. equiv. of the stoppers, 0.25 equiv. of dibenzo-18-crown-6, and an excess of $K_2CO_3$ for six days (depending on the deslipping rate, it was in some cases beneficial to terminate the reaction somewhat earlier). After removal of the solvent, the rotaxane was purified by column chromatography with $CH_2Cl_2$/ethyl acetate mixtures on silica gel.

***Rot7@2:*** **[2]{1,4-Bis(3,5-di-*tert*-butylphenyloxymethyl)benzene}-{11′-*tert*-butyl-5′,17′,23′,35′,38′,40′,43′,45′-octamethyldispiro[cyclohexane-1,2′-7′,15′,25′,33′-tetraazaheptacyclo-[32.2.2.2$^{3'.6'}$.2$^{16'.19'}$.2$^{21'.24'}$.1$^{9'.13'}$.1$^{27'.31'}$]hexatetraconta3′,5′,9′,11′,13′(44′),16′,18′,21′,23′,27′,29′,31′(39′),34′,36′,37′,40′,42′,45′-octadecaene-20′,1′′-cyclohexane]-8′,14′,26′,32′-tetrone}rotaxane:** $R_f$ = 0.20 ($CH_2Cl_2$/MeOH = 30:1); yield: 37%. − $^1$H NMR (250 MHz, $CDCl_3$) δ (ppm) = 1.35 [s, 36 H, C(CH$_3$)$_3$], 1.38 [s, 9 H, C(CH$_3$)$_3$], 1.55 (br. s, 4 H, CH$_2$), 1.68 (br. s, 8 H, CH$_2$), 1.85 (s, 12 H, Ar-CH$_3$), 1.88 (s, 12 H, Ar-CH$_3$), 2.32 (br. s, 8 H, CH$_2$), 4.33 (s, 4 H, OCH$_2$), 5.81 (s, 4 H, Ar-H), 7.01 (s, 4 H, Ar-H), 7.02 (s, 4 H, Ar-H), 7.05 (s, 2 H, Ar-H), 7.45 (s, 2 H, NH), 7.50 (s, 2 H, NH), 7.65 (t, $^3J$ = 8.6 Hz, 1 H, Ar-H), 7.75 (s, 1 H, Ar-H), 7.92 (s, 1 H, Ar-H), 8.20 (d, $^3J$ = 8.6 Hz, 2 H, Ar-H), 8.22 (s, 2 H, Ar-H). − $^{13}$C NMR (62.5 MHz, $CDCl_3$) δ (ppm) = 18.5, 18.6, 23.0, 26.3, 31.2, 31.3, 34.8, 35.2, 35.7, 45.2, 71.3, 108.8, 116.6, 122.1, 124.7, 126.8, 126.9, 127.8, 129.6, 130.4, 131.1, 131.2, 132.4, 134.2, 134.4, 135.1, 135.9, 149.0, 153.1, 154.0, 157.7, 165.3, 165.7. − MALDI-TOF-MS: *m*/*z* (%) = 1498.3 (100) [M + Na$^+$].

***Rot8@2:*** **[2]{4,4′-Bis(3,5-di-*tert*-butylphenyloxymethyl)biphenyl}-{11′-*tert*-butyl-5′,17′,23′,35′,38′,40′,43′,45′-octamethyldispiro[cyclohexane-1,2′-7′,15′,25′,33′-tetraazaheptacyclo-[32.2.2.2$^{3'.6'}$.2$^{16'.19'}$.2$^{21'.24'}$.1$^{9'.13'}$.1$^{27'.31'}$]hexatetraconta-3′,5′,9′,11′,13′(44′),16′,18′,21′,23′,27′,29′,31′(39′),34′,36′,37′,40′,42′,45′-octadecaene-20′,1′′-cyclohexane]-8′,14′,26′,32′-tetrone}rotaxane:** $R_f$ = 0.22 ($CH_2Cl_2$/MeOH = 30:1); yield: 42%. − $^1$H NMR (250 MHz, $C_2D_2Cl_4$) δ (ppm) = 1.25 [s, 36 H, C(CH$_3$)$_3$], 1.35 [s, 9 H, C(CH$_3$)$_3$], 1.57 (br. s, 4 H, CH$_2$), 1.71 (br. s, 8 H, CH$_2$), 1.96 (s, 24 H, Ar-CH$_3$), 2.36 (br. s, 8 H, CH$_2$), 4.79 (s, 4 H, OCH$_2$), 6.45 (d, $^3J$ = 7.9 Hz, 4 H, Ar-H), 6.65 (s, 4 H, Ar-H), 6.69 (d, $^3J$ = 7.9 Hz, 4 H, Ar-H), 6.94 (s, 2 H, Ar-H), 6.99 (s, 2 H, NH), 7.06 (s, 2 H, NH), 7.10 (s, 8 H, Ar-H), 7.35 (s, 1 H, Ar-H), 7.49 (s, 1 H, Ar-H), 7.61 (t, $^3J$ = 7.7 Hz, 1 H, Ar-H), 8.15 (d, $^3J$ = 7.7 Hz, 2 H, Ar-H), 8.20 (s, 2 H, Ar-H). − $^{13}$C NMR (62.5 MHz, $CDCl_3$) δ (ppm) = 23.1, 26.3, 29.2, 29.5, 29.6, 31.4, 31.9, 34.9, 36.2, 45.4, 70.1, 108.8, 115.9, 121.6, 124.1, 124.7, 127.2, 127.3, 128.5, 129.6, 129.7, 130.3, 131.1, 131.4, 132.3, 134.1, 134.6, 134.9, 135.9, 137.8, 149.2, 164.3, 165.6. − MALDI-TOF-MS: *m*/*z* (%) = 1576.2 (95) [M + Na$^+$].

***Rot9@2:*** **[2]{4,4′-Bis(3,5-di-*tert*-butylphenyloxymethyl)-1,1′-bibenzyl}-{11′-*tert*-butyl-5′,17′,23′,35′,38′,40′,43′,45′-octamethyldispiro[cyclohexane-1,2′-7′,15′,25′,33′-tetraazaheptacyclo-[32.2.2.2$^{3'.6'}$.2$^{16'.19'}$.2$^{21'.24'}$.1$^{9'.13'}$.1$^{27'.31'}$]hexatetraconta-3′,5′,9′,11′,13′(44′),16′,18′,21′,23′,27′,29′,31′(39′),34′,36′,37′,40′,42′,45′-octadecaene-20′,1′′-cyclohexane]-8′,14′,26′,32′-tetrone}rotaxane:** $R_f$ = 0.89 ($CH_2Cl_2$/MeOH = 20:1); yield: 57%; m.p. 206−208 °C. − $^1$H NMR (250 MHz, $C_2D_2Cl_4$) δ (ppm) = 1.24 [s, 36 H, C(CH$_3$)$_3$], 1.41 [s, 9 H, C(CH$_3$)$_3$], 1.60 (br, 8 H, CH$_2$), 1.74 (br. s, 8 H, CH$_2$), 1.95 (s, 12 H, Ar-CH$_3$), 1.96 (s, 12 H, Ar-CH$_3$), 2.42 (br. s, 8 H, CH$_2$), 4.56 (s, 4 H, OCH$_2$), 6.47 (d, $^3J$ = 7.7 Hz, 4 H, Ar-H), 6.61 (d, $^3J$ = 7.7 Hz, 4 H, Ar-H), 6.64 (s, 4 H, Ar-H), 7.02 (s, 2 H, Ar-H), 7.04 (s, 4 H, NH), 7.11 (s, 8 H, Ar-H), 7.55 (s, 1 H, Ar-H), 7.70 (s, 1 H, Ar-H), 7.72 (t, $^3J$ = 7.6 Hz, 1 H, Ar-H), 8.16 (d, $^3J$ = 7.6 Hz, 2 H, Ar-H), 8.18 (s, 2 H, Ar-H). − $^{13}$C NMR (62.5 MHz, $CDCl_3$) δ (ppm) = 18.8, 23.0, 26.3, 31.1, 31.3, 34.9, 35.3, 35.7, 37.6, 45.3, 70.0, 108.8, 115.7, 121.5, 124.2, 126.2, 126.8, 127.9, 128.6, 129.4, 130.3, 131.0, 131.1, 132.1, 134.4, 134.5, 134.7, 134.8, 140.8, 148.6, 148.7, 152.6, 154.2, 157.9, 165.0, 165.4. − FAB-MS: *m*/*z* (%) = 1580.6 (55) [M + H$^+$].

***Rot10@2′:*** **[2]{1,4-Bis(3,5-diphenylphenyloxymethyl)benzene}-{11′,29′-di-*tert*-butyl-5′,17′,23′,35′,38′,40′,43′,45′-octamethyldispiro[cyclohexane-1,2′-7′,15′,25′,33′-tetraazaheptacyclo[32.2.2.2$^{3'.6'}$.2$^{16'.19'}$.2$^{21'.24'}$.1$^{9'.13'}$.1$^{27'.31'}$]hexatetraconta-3′,5′,9′,11′,13′(44′),16′,18′,21′,23′,27′,29′,31′(39′),34′,36′,37′,40′,42′,45′-octadecaene-20′,1′′-cyclohexane]-8′,14′,26′,32′-tetrone}rotaxane:** $R_f$ = 0.20 ($CH_2Cl_2$/MeOH = 100:1); yield: 17%. − $^1$H NMR (500 MHz, $CDCl_3$) δ (ppm) = 1.27 [s, 18 H, C(CH$_3$)$_3$], 1.56 (br, 4 H, CH$_2$), 1.70 (br. s, 8 H, CH$_2$), 1.94 (s, 24 H, Ar-CH$_3$), 2.34 (br. s, 8 H, CH$_2$), 4.56 (s, 4 H, OCH$_2$), 6.45 (d, $^3J$ = 8.2 Hz, 2 H, Ar-H), 6.78 (d, $^3J$ = 8.2 Hz, 2 H, Ar-H), 7.00 (s, 8 H, Ar-H), 7.05 (s, 4 H, Ar-H), 7.10 (br. s, 2 H, Aryl-H), 7.28 (s, 4 H, Aryl-H), 7.39 (m, br, 16 H, Ar-H), 7.44 (m, br, 16 H, Ar-H), 7.64 (s, 2 H, Ar-H), 8.19 (s, 4 H, Ar-H). − $^{13}$C NMR (125 MHz, $CDCl_3$) δ (ppm) = 19.1, 23.4, 26.7, 31.4, 32.8, 35.1, 45.7, 70.3, 113.4, 127.3, 127.4, 127.6, 127.8, 128.0, 128.4, 129.1, 129.3, 131.5, 134.5, 135.1, 136.7, 141.2, 143.6, 143.7, 156.7, 159.2, 166.2. − MALDI-TOF-MS: *m*/*z* (%) = 1650.7 (55) [M + K$^+$].

***Rot11@2′:*** **[2]{4,4′-Bis(3,5-diphenylphenyloxymethyl)-1,1′-bibenzyl}-{11′,29′-di-*tert*-butyl-5′,17′,23′,35′,38′,40′,43′,45′-octamethyldispiro[cyclohexane-1,2′-7′,15′,25′,33′-tetraazaheptacyclo[32.2.2.2$^{3'.6'}$.2$^{16'.19'}$.2$^{21'.24'}$.1$^{9'.13'}$.1$^{27'.31'}$]hexatetraconta-3′,5′,9′,11′,13′(44′),16′,18′,21′,23′,27′,29′,31′(39′),34′,36′,37′,40′,42′,45′-octadecaene-20′,1′′-cyclohexane]-8′,14′,26′,32′-tetrone}rotaxane:** $R_f$ = 0.23 ($CH_2Cl_2$/MeOH = 100:1); yield: 19%. − $^1$H NMR (500 MHz, $CDCl_3$) δ (ppm) = 1.43 [s, 18 H, C(CH$_3$)$_3$], 1.59 (br. s, 4 H, CH$_2$), 1.72 (br. s, 8 H, CH$_2$), 2.07 (s, 24 H, Ar-CH$_3$), 2.38 (br. s, 8 H, CH$_2$), 2.44 (s, 4 H, C$_2$H$_4$), 4.81 (s, 4 H, OCH$_2$), 6.44 (d, $^3J$ = 8.0 Hz, 4 H, Ar-H), 6.71 (d, $^3J$ = 8.0 Hz, 4 H, Ar-H), 7.04 (s, 8 H, Ar-H), 7.09 (s, 4 H, Ar-H), 7.28 (s, 4 H, N−H), 7.40 (m, br, 16 H, Ar-H), 7.46 (m, br, 16 H, Ar-H), 7.56 (s, 2 H, Ar-H), 7.57 (s, 4 H, Ar-H), 8.20 (s, 4 H, Ar-H). − $^{13}$C NMR (125 MHz, $CDCl_3$) δ (ppm) = 19.3, 22.7, 26.7, 31.5, 34.5, 36.1, 38.1, 45.7, 70.9, 112.7, 127.3, 127.5, 127.6, 127.9, 128.2, 128.5, 129.1, 129.2, 129.3, 129.8, 131.5, 134.6, 134.8, 135.1, 141.0, 143.8, 145.2, 154.6, 159.5, 165.9. − MALDI-TOF-MS: *m*/*z* (%) = 1737.7 (90) [M + Na$^+$].

**General Procedure for the Synthesis of Amide Rotaxanes:** Equimolar amounts of the macrocycle and 4,4′-biphenyldicarboxylic acid dichloride were treated with the stopper amine and 2 equiv. triethyl-

amine in dichloromethane. The stopper was added by perfusor over 8 hours. After complete addition, the mixture was stirred at room temperature for 36 hours, the solvent was then removed, and the residue was purified by column chromatography on silica gel with $CH_2Cl_2$/ethyl acetate mixtures.

***Macrocycle 14:*** **3,3′′,5′,17′,23′,35′,38′,40′,43′,45′-decamethyldispiro-[cyclohexane-1,2′-7′,15′,25′,33′,39′,44′-hexaazaheptacyclo-[32.2.2.2$^{3'.6'}$.2$^{16'.19'}$.2$^{21'.24'}$.1$^{9'.13'}$.1$^{27'.31'}$]hexatetraconta-3′,5′,9′,11′,13′(44′),16′,18′,21′,23′,27′,29′,31′(39′),34′,36′,37′,40′,42′,45′-octadecaene-20′,1′′-cyclohexane]-8′,14′,26′, 32′-tetrone:** The macrocycle was a mixture of *syn*/*anti* isomers with respect to the two methyl groups at the cyclohexyl rings. Some of the NMR signals therefore appear as a double set. − $R_f$ = 0.43 ($CH_2Cl_2$/EtOAc = 8:1); yield: 29%; m.p. > 300 °C. − $^1$H NMR (400 MHz, $CDCl_3$) δ (ppm) = 0.91−0.99 (br. s, 6 H, $CH_3$), 1.41−1.50 (m, 2 H, $CH_2$), 1.55−1.75 (m, 10 H, $CH_2$), 2.15−2.22 (m, 24 H, $CH_3$), 2.57−2.75 (m, 4 H, $CH_2$), 6.91 (s, 2 H, Ar-H), 6.93 (s, 2 H, Ar-H), 6.98 (s, 4 H, Ar-H), 8.12−8.17 (m, 2 H, Ar-H), 8.44−8.50 (m, 4 H, ArH), 8.96 (s, 1 H, NH), 9.02 (s, 1 H, NH), 9.05 (s, 1 H, NH), 9.09 (s, 1 H, NH). − $^{13}$C NMR (100.6 MHz, $CDCl_3$) δ (ppm) = 18.9, 19.0, 23.0 ($CH_3$), 22.7, 22.8, 35.0, 35.1, 35.6, 44.8 ($CH_2$), 28.4, 28.5, 125.2, 125.3, 125.4, 125.8, 125.9, 127.4, 127.5, 127.8, 139.7, 139.8 (CH), 45.6, 45.7, 130.3, 130.4, 130.5, 134.3, 134.4, 134.9, 135.0, 146.2, 148.2, 148.5, 148.6, 150.9 151.0 (Cq), 160.9, 161.0, 161.1, 161.2 (CO). − MALDI-MS: *m*/*z* (%) = 958.3 (100) [M + $Na^+$]. − $C_{60}H_{66}N_6O_4{\cdot}H_2O$ (935.20): calcd. C 75.60, H 7.19 N 8.81, found C 75.75 H 7.00 N 8.62.

***Rot3@13:*** **[2]{*N*,*N*′-Bis[3,5-di(*tert*-butyl)phenyl]-1,1′-biphenyl-4,4′dicarboxamide}-{11′-*tert*-butyl-5′,17′,23′,35′,38′,40′,43′,45′-octamethyldispiro[cyclohexane-1,2′-7′,15′,25′,33′,39′-pentaazaheptacyclo-[32.2.2.2$^{3'.6'}$.2$^{16'.19'}$.2$^{21'.24'}$.1$^{9'.13'}$.1$^{27'.31'}$]hexatetraconta-3′,5′,9′,11′,13′(44′),16′,18′,21′,23′,27′,29′,31′(39′),34′,36′,37′,40′,42′,45′-octadecaene-20′,1′′-cyclohexane]-8′,14′,26′,32′-tetrone}rotaxane.** $R_f$ = 0.87 ($CH_2Cl_2$/EtOAc = 10:1); yield: 3%; m.p. > 300 °C. − $^1$H NMR (500 MHz, [D$_7$]DMF) δ (ppm) = 1.30 [s, 36 H, C($CH_3$)$_3$], 1.37 [s, 9 H, C($CH_3$)$_3$], 1.47−1.57 (br. s, 4 H, $CH_2$), 1.58−1.69 (br. s, 8 H, $CH_2$), 1.96 (s, 12 H, $CH_3$), 2.06 (s, 12, $CH_3$), 2.32−2.58 (br. s, 8 H, $CH_2$), 7.24−7.27 (m, 6 H, Ar-H), 7.28 (s, 8 H, Ar-H), 7.35 (br, 4 H, Ar−H, NH), 7.65 (s, 3 H, Ar-H), 8.02 (s, 6 H, Ar-H), 8.15 (br. s, 1 H, NH), 8.33−8.40 (m, 3 H, Ar-H), 8.76 (s, 1 H, NH), 9.22 (br. s, 1 H, NH), 10.22 (br. s, 1 H, NH). − $^{13}$C NMR (100.6 MHz, $CD_2Cl_2$/$CD_3OD$) δ (ppm) = 18.2, 18.4, 30.9 ($CH_3$), 23.1, 26.3, 36.1 ($CH_2$), 114.7, 119.4, 123.6, 125.7, 126.7, 126.9, 127.5, 128.5 (CH), 34.9, 45.4, 118.4, 126.9, 130.5, 131.6, 134.5, 134.8, 135.3, 136.1, 137.2, 140.2, 142.2, 148.4, 148.6, 149.8, 152.1 154.1 (Cq), 161.6, 166.4, 166.7 (CO). − MALDI-MS: *m*/*z* (%) = 1602.9 (100) [M + $Na^+$].

***Rot3@14:*** **[2]{*N*,*N*′-Bis[3,5-di(*tert*-butyl)phenyl]-1,1′-biphenyl-4,4′dicarboxamide}-{3,3′′,5′,17′,23′,35′,38′,40′,43′,45′-decamethyldispiro[cyclohexane-1,2′-7′,15′,25′,33′,39′,44′-hexaazaheptacyclo-[32.2.2.2$^{3'.6'}$.2$^{16'.19'}$.2$^{21'.24'}$.1$^{9'.13'}$.1$^{27'.31'}$]hexatetraconta-3′,5′,9′,11′,13′(44′),16′,18′,21′,23′,27′,29′,31′(39′),34′,36′,37′,40′,42′,45′-octadecaene-20′,1′′-cyclohexane]-8′,14′,26′,32′-tetrone}rotaxane:** The rotaxane was a mixture of *syn*/*anti* isomers with respect to the two methyl groups at the cyclohexyl rings. Some of the NMR signals therefore appear as a double set. − $R_f$ = 0.31 ($CH_2Cl_2$/EtOAc = 20:1); yield: 2%; m.p. > 300 °C. − $^1$H NMR (500 MHz, $CDCl_3$) δ (ppm) = 0.88−0.98 (br. s, 6 H, $CH_3$), 1.30 [s, 36 H, C($CH_3$)$_3$], 1.33−1.36 (m, 6 H, $CH_3$), 1.37−1.41 (m, 3 H, $CH_3$), 1.54−1.59 (m, 6 H, $CH_3$), 1.62−1.78 (m, 10 H, $CH_2$), 1.79−1.91 (m, 6 H, $CH_3$), 2.21−2.34 (m, 3 H, $CH_3$), 2.54−2.71 (m, 4 H, $CH_2$), 6.64−6.71 (m, 4 H, Ar-H), 6.72 (s, 4 H, Ar-H), 6.78−6.88 (m, 4 H, Ar-H), 6.99 (s, 4 H, ArH), 7.47−7.54 (m, 6 H, Ar-H), 7.73 (d, $^3J$ = 8.2 Hz, 4 H, ArH), 7.98 (d, $^3J$ = 8.2 Hz, 4 H, ArH), 8.10−8.17 (m, 2 H, Ar-H), 8.36−8.54 (m, 4 H, Ar-H), 8.89 (s, 1 H, NH), 8.92 (s, 1 H, NH), 9.64 (s, 1 H, NH), 9.74 (s, 1 H, NH). − $^{13}$C NMR (125.8 MHz, $CDCl_3$) δ (ppm) = 18.4, 19.0, 19.6, 23.4, 31.8 ($CH_3$), 23.1, 23.3, 29.7, 30.0, 30.1, 35.4, 45.3, 45.4 ($CH_2$), 28.9, 29.0, 114.5, 115.2, 119.4, 125.7, 125.8, 126.3, 126.4, 126.9, 127.5, 127.9, 128.1, 128.8, 139.8, 140.0, 140.1 (CH), 29.7, 46.1, 46.3, 131.9, 135.4, 136.0, 136.3, 137.6, 147.6, 149.1, 152.2, 152.3, 152.4 (Cq), 161.1, 161.3, 161.8, 162.0 (CO). − MALDI-MS: *m*/*z* (%) = 1578.8 (100) [M + $Na^+$].

## Acknowledgments

We warmly thank Prof. Fritz Vögtle for valuable advice, Dr. Jens Windscheidt, and Dr. Annette Hünten for their help in the synthesis of the rotaxanes, and Dr. Heinz-Rudolf Hartmann and Ulrike Weynand for recording the 2D NMR spectra and the generous supply of instrument time for the NMR kinetics experiments. C.A.S. thanks the Fonds der Chemischen Industrie for a Liebig fellowship. This work was funded in part by the Deutsche Forschungsgemeinschaft.

[1] [1a] G. Schill, *Catenanes, Rotaxanes and Knots*, Academic Press, New York, **1971**. − [1b] *Molecular Catenanes, Rotaxanes, and Knots* (Eds.: J. P. Sauvage, C. Dietrich-Buchecker), Wiley-VCH, Weinheim, **1999**.

[2] For a recent example of a knot synthesis based on nonionic template effects, see: O. Safarowsky, M. Nieger, R. Fröhlich, F. Vögtle, *Angew. Chem.* **2000**, *112*, 1699−1701; *Angew. Chem. Int. Ed.* **2000**, *39*, 1616−1618.

[3] For reviews, see: [3a] C. O. Dietrich-Buchecker, J.-P. Sauvage, *Chem. Rev.* **1987**, *87*, 795−810. − [3b] J.-P. Sauvage, *Acc. Chem. Res.* **1990**, *23*, 319−327. − [3c] S. Anderson, H. L. Anderson, J. K. M. Sanders, *Acc. Chem. Res.* **1993**, *26*, 469−475. − [3d] R. Hoss, F. Vögtle, *Angew. Chem.* **1994**, *106*, 389−398; *Angew. Chem. Int. Ed. Engl.* **1994**, *33*, 375−384. − [3e] J.-C. Chambron, C. O. Dietrich-Buchecker, V. Heitz, J.-F. Nierengarten, J.-P. Sauvage, C. Pascard, J. Guilhem, *Pure Appl. Chem.* **1995**, *67*, 233−240. − [3f] R. Jäger, F. Vögtle, *Angew. Chem.* **1997**, *109*, 966−980; *Angew. Chem. Int. Ed. Engl.* **1997**, *36*, 930−944. − [3g] S. A. Nepogodiev, J. F. Stoddart, *Chem. Rev.* **1998**, *98*, 1959−1976. − [3h] F. M. Raymo, J. F. Stoddart, *Chem. Rev.* **1999**, *99*, 1043−1063.

[4] [4a] D. E. Adams, E. M. Shekhtman, E. L. Zechiedrich, M. B. Schmid, N. R. Cozzarelli, *Cell* **1992**, *71*, 277−288. − [4b] J. Chen, C. A. Rauch, J. H. White, P. T. Englund, N. R. Cozzarelli, *Cell* **1995**, *80*, 61−69. − For a review, see: [4c] N. C. Seeman, *Angew. Chem.* **1998**, *110*, 3408−3428; *Angew. Chem. Int. Ed.* **1998**, *37*, 3220−3238.

[5] [5a] C. Liang, K. Mislow, *J. Am. Chem. Soc.* **1994**, *116*, 11189−11190. − [5b] F. Takusagawa, S. Kamitori, *J. Am. Chem. Soc.* **1996**, *118*, 8945−8946.

[6] [6a] P. D. Boyer, *Angew. Chem.* **1998**, *110*, 2424−2436; *Angew. Chem. Int. Ed.* **1998**, *37*, 2296−2307. − [6b] J. E. Walker, *Angew. Chem.* **1998**, *110*, 2438−2450; *Angew. Chem. Int. Ed.* **1998**, *37*, 2308−2319.

[7] R. M. Macnab, S.-I. Aizawa, *Annu. Rev. Biophys. Bioeng.* **1984**, *13*, 51−83.

[8] [8a] D. K. Mitchell, J.-P. Sauvage, *Angew. Chem.* **1988**, *100*, 985−987; *Angew. Chem. Int. Ed. Engl.* **1988**, *27*, 930−932. − [8b] Y. Kaida, Y. Okamoto, J.-C. Chambron, D. K. Mitchell, J.-P. Sauvage, *Tetrahedron Lett.* **1993**, *34*, 1019−1023. − [8c] P. R. Ashton A. S. Reder, N. Spencer, J. F. Stoddart, *J. Am. Chem. Soc.* **1993**, *115*, 5286−5287. − [8d] C. Yamamoto, Y. Okamoto, T. Schmidt, R. Jäger, F. Vögtle, *J. Am. Chem. Soc.* **1997**, *119*, 10547−10548. − [8e] P. R. Ashton, J. A. Bravo, F. M. Raymo,

J. F. Stoddart, A. J. P. White, D. J. Williams, *Eur. J. Org. Chem.* **1999**, 899−908. − [8f] R. Schmieder, G. Hübner, C. Seel, F. Vögtle, *Angew. Chem.* **1999**, *111*, 3741−3743; *Angew. Chem. Int. Ed.* **1999**, *38*, 3528−3530. − [8g] C. Reuter, A. Mohry, A. Sobanski, F. Vögtle, *Chem. Eur. J.* in press. − For a review, see: [8h] J.-C. Chambron, C. O. Dietrich-Buchecker, J. P. Sauvage, *Top. Curr. Chem.* **1993**, *165*, 131−162.

[9] [9a] K. E. Drexler, *Annu. Rev. Biophys. Biomol. Struct.* **1994**, *23*, 377−405. − [9b] V. Balzani, M. Gómez-López, J. F. Stoddart, *Acc. Chem. Res.* **1998**, *31*, 405−413. − [9c] J.-P. Sauvage, *Acc. Chem. Res.* **1998**, *31*, 611−619. − [9d] J.-P. Collin, P. Gaviña, V. Heitz, J.-P. Sauvage, *Eur. J. Inorg. Chem.* **1998**, 1−14. − [9e] Z. Asfari, J. Vicens, *J. Incl. Phenom. Macrocyc. Chem.* **2000**, *36*, 103−118. − [9f] V. Balzani, A. Credi, F. M. Raymo, J. F. Stoddart, *Angew. Chem.* **2000**, *112*, 3484−3530; *Angew. Chem. Int. Ed.* **2000**, *39*, 3348−3391. − [9g] C. A. Schalley, K. Beizai, F. Vögtle, *Acc. Chem. Res.* submitted.

[10] [10a] D. J. Cárdenas, P. Gaviñas, J.-P. Sauvage, *Chem. Commun.* **1996**, 1915−1916. − [10b] D. B. Amabilino, C. O. Dietrich-Buchecker, J.-P. Sauvage, *J. Am. Chem. Soc.* **1996**, *118*, 3285−3286. − [10c] D. J. Cárdenas, P. Gaviñas, J.-P. Sauvage, *J. Am. Chem. Soc.* **1997**, *119*, 2656−2664. − For a review, see: [10d] J.-C. Chambron, S. Chardon-Noblat, A. Harriman, V. Heitz, J.-P. Sauvage, *Pure Appl. Chem.* **1993**, *65*, 2343−2349.

[11] F. Diederich, L. Echegoyen, M. Gómez-López, R. Kessinger, J. F. Stoddart, *J. Chem. Soc., Perkin Trans. 2* **1999**, 1577−1586.

[12] F. Vögtle, W. M. Müller, U. Müller, M. Bauer, K. Rissanen, *Angew. Chem.* **1993**, *105*, 1356−1358; *Angew. Chem. Int. Ed. Engl.* **1993**, *32*, 1295−1297.

[13] S. S. Zhu, P. J. Carroll, T. M. Swager, *J. Am. Chem. Soc.* **1996**, *118*, 8713−8714.

[14] [14a] A. Credi, V. Balzani, S. J. Langford, J. F. Stoddart, *J. Am. Chem. Soc.* **1997**, *119*, 2679−2681. − [14b] M. Asakawa, P. R. Ashton, V. Balzani, A. Credi, G. Mattersteig, O. A. Matthews, M. Montalti, N. Spencer, J. F. Stoddart, M. Venturi, *Chem. Eur. J.* **1997**, *3*, 1992−1996.

[15] For a computational study of the size requirements of the deslipping process, see: F. M. Raymo, K. N. Houk, J. F. Stoddart, *J. Am. Chem. Soc.* **1998**, *120*, 9318−9322.

[16] [16a] G. Hübner, G. Nachtsheim, Q.-Y. Li, C. Seel, F. Vögtle, *Angew. Chem.* **2000**, *112*, 1315−1318; *Angew. Chem. Int. Ed.* **2000**, *39*, 1269−1272. − Also, see: [16b] H. W. Gibson, S. Liu, P. Lecavalier, C. Wu, Y. X. Shen, *J. Am. Chem. Soc.* **1995**, *117*, 852−874. − [16c] C. Heim, Ph. D. Thesis, Universität Bonn, **1998**. − [16d]C. Heim, A. Affeld, M. Nieger, F. Vögtle, *Helv. Chim. Acta* **1999**, *82*, 746−759.

[17] [17a] P. R. Ashton, R. Ballardini, V. Balzani, M. Blohradský, M. T. Gandolfi, D. Philp, L. Prodi, F. M. Raymo, M. V. Reddington, N. Spencer, J. F. Stoddart, M. Venturi, D. J. Williams, *J. Am. Chem. Soc.* **1996**, *118*, 4931−4951. − [17b] M. Asakawa, P. R. Ashton, R. Ballardini, V. Balzani, M. Bělohradský, M. T. Gandolfi, O. Kocian, L. Prodi, F. M. Raymo, J. F. Stoddart, M. Venturi, *J. Am. Chem. Soc.* **1997**, *119*, 302−310. − [17c] P.R. Ashton, I. Baxter, M. C. T. Fyfe, F. M. Raymo, N. Spencer, J. F. Stoddart, A. J. P. White, D. J. Williams, *J. Am. Chem. Soc.* **1998**, *120*, 2297−2307.

[18] For a study of binding constants of the pseudorotaxane axles in the corresponding wheels, see: [18a] P. R. Ashton, D. Philp, M. V. Reddington, A. M. Z. Slawin, N. Spencer, J. F. Stoddart, D. J. Williams, *J. Chem. Soc., Chem. Commun.* **1991**, 1680−1682. − For some recent publications on pseudorotaxanes, see: [18b] P. R. Ashton, M. C. T. Fyfe, M.-V. Martínez-Díaz, S. Menzer, C. Schiavo, J. F. Stoddart, A. J. P. White, D. J. Williams, *Chem. Eur. J.* **1998**, *4*, 1523−1534. − [18c] C. Gong, H. W. Gibson, *Angew. Chem.* **1998**, *110*, 323−327; *Angew. Chem. Int. Ed.* **1998**, *37*, 310−314. − [18d] P. R. Ashton, I. W. Parsons, F. M. Raymo, J. F. Stoddart, A. J. P. White, D. J. Williams, R. Wolf, *Angew. Chem.* **1998**, *110*, 2016−2019; *Angew. Chem. Int. Ed.* **1998**, *37*, 1913−1916.

[19] [19a] I. T. Harrison, *J. Chem. Soc., Chem. Commun.* **1972**, 231−232. − [19b] I. T. Harrison, *J. Chem. Soc., Perkin Trans. 1* **1974**, 301−304. − [19c] G. Agam, D. Graiver, A. Zilkha, *J. Am. Chem. Soc.* **1976**, *98*, 5206−5214. − [19d] G. Agam, A. Zilkha, *J. Am. Chem. Soc.* **1976**, *98*, 5214−5216. − [19e] G. Schill, W. Beckmann, N. Schweickert, H. Fritz, *Chem. Ber.* **1986**, *119*, 2647−2655. − [19f] P. R. Ashton, M. Belohradský, D. Philp, J. F. Stoddart, *J. Chem. Soc., Chem. Commun.* **1993**, 1269−1274. − [19g] P. R. Ashton, M. Belohradský, D. Philp, N. Spencer, J. F. Stoddart, *J. Chem. Soc., Chem. Commun.* **1993**, 1274−1277. − [19h] D. H. Macartney, *J. Chem. Soc., Perkin Trans. 2* **1996**, 2775−2778. − [19i] M. Händel, M. Plevoets, S. Gestermann, F. Vögtle, *Angew. Chem.* **1997**, *109*, 1248−1250; *Angew. Chem. Int. Ed. Engl.* **1997**, *36*, 1199−1201. − [19j] M. C. T. Fyfe, F. M. Raymo, J. F. Stoddart, in: *Stimulating Concepts in Chemistry* (Eds.: J. F. Stoddart, F. Vögtle), Wiley-VCH, Weinheim, **2000**, p. 211.

[20] For a few examples, see: [20a] P. L. Anelli, N. Spencer, J. F. Stoddart, *J. Am. Chem. Soc.* **1991**, *113*, 5131−5133. − [20b] R. A. Bissell, E. Córdova, A. E. Kaifer, *Nature* **1994**, *369*, 133−137. − [20c] D. B. Amabilino, P.-L. Anelli, P. R. Ashton, G. R. Brown, E. Córdova, L. A. Godínez, W. Hayes, A. E. Kaifer, D. Philp, A. M. Z. Slawin, N. Spencer, J. F. Stoddart, M. S. Tolley, D. J. Williams, *J. Am. Chem. Soc.* **1995**, *117*, 11142−11170. − [20d] A. C. Benniston, A. Harriman, V. M. Lynch, *J. Am. Chem. Soc.* **1995**, *117*, 5275−5291. − [20e] A. S. Lane, D. A. Leigh, A. Murphy, *J. Am. Chem. Soc.* **1997**, *119*, 11092−11093. − [20f] J.-P. Collin, P. Gaviña, J.-P. Sauvage, *New J. Chem.* **1997**, *21*, 525−528. − [20g] H. Murakami, A. Kawabuchi, K. Kotoo, M. Kunitake, M. Nakashima, *J. Am. Chem. Soc.* **1997**, *119*, 7605−7606. − [20h] D. A. Leigh, A. Troisi, F. Zerbetto, *Angew. Chem.* **2000**, *112*, 358−361; *Angew. Chem. Int. Ed.* **2000**, *39*, 350−353.

[21] For a small selection of references, see: [21a] A. Livoreil, C. O. Dietrich-Buchecker, J.-P. Sauvage, *J. Am. Chem. Soc.* **1994**, *116*, 9399−9400. − [21b] A. G. Johnston, D. A. Leigh, R. J. Pritchard, M. D. Deegan, *Angew. Chem.* **1995**, *107*, 1324−1327; *Angew. Chem. Int. Ed. Engl.* **1995**, *34*, 1209−1212. − [21c] D. A. Leigh, K. Moody, J. P. Smart, K. J. Watson, A. M. Z. Slawin, *Angew. Chem.* **1996**, *108*, 326−331; *Angew. Chem. Int. Ed. Engl.* **1996**, *35*, 306−310. − [21d] F. Vögtle, T. Dünnwald, T. Schmidt, *Acc. Chem. Res.* **1996**, *29*, 451−460. − [21e] A. Livoreil, J.-P. Sauvage, N. Armaroli, V. Balzani, L. Flamigni, B. Ventura, *J. Am. Chem. Soc.* **1997**, *119*, 12114−12124. − [21f] M. C. T. Fyfe, P. T. Glink, S. Menzer, J. F. Stoddart, A. J. P. White, D. J. Williams, *Angew. Chem.* **1997**, *109*, 2158−2160; *Angew. Chem. Int. Ed. Engl.* **1997**, *36*, 2068−2070. − [21g] M. S. Deleuze, D. A. Leigh, F. Zerbetto, *J. Am. Chem. Soc.* **1999**, *121*, 2364−2379.

[22] C. Seel, A. H. Parham, O. Safarowsky, G. M. Hübner, F. Vögtle, *J. Org. Chem.* **1999**, *64*, 7236−7242.

[23] [23a] C. Reuter, C. Seel, M. Nieger, F. Vögtle, *Helv. Chim. Acta* **2000**, *83*, 630−640. − [23b] A. Mohry, F. Vögtle, M. Nieger, H. Hupfer, *Chirality* **2000**, *12*, 76−83.

[24] **Rot10@2′** and **Rot11@2′** both bear an additional *tert*-butyl group at the periphery of the wheel. We believe that it does not significantly alter the deslipping kinetics. If so, one would expect some additional steric hindrance, which, however, is not in line with the results in Table 1.

[25] B. Sunners, L. H. Piette, W. G. Schneider, *Can. J. Chem.* **1960**, *38*, 681−688.

[26] [26a] K. B. Wiberg, K. E. Laidig, *J. Am. Chem. Soc.* **1987**, *109*, 5935−5943. − [26b] For a review, see: K. B. Wiberg, C.M. Hadad, C. M. Breneman, K. E. Laidig, M. A. Murcko, T. J. LePage, *Science* **1991**, *252*, 1266−1272.

[27] C. M. Breneman, L. W. Weber, *Can. J. Chem.* **1996**, *74*, 1271−1282.

[28] D. A. Leigh, A. Murphy, J. P. Smart, A. M. Z. Slawin, *Angew. Chem.* **1997**, *109*, 752−756; *Angew. Chem. Int. Ed. Engl.* **1997**, *36*, 728−732.

[29] S. Ottens−Hildebrandt, M. Nieger, K. Rissanen, J. Rouvinen, S. Meier, G. Harder, F. Vögtle, *J. Chem. Soc., Chem. Commun.* **1995**, 777−778.

[30] A. G. Johnston, D. A. Leigh, L. Nehzat, J. P. Smart, M. D. Deegan, *Angew. Chem.* **1995**, *107*, 1327−1331; *Angew. Chem. Int. Ed. Engl.* **1995**, *34*, 1202−1216.

[31] [31a] Y. Hamuro, S. J. Geib, A. D. Hamilton, *Angew. Chem.* **1994**, *106*, 465−467; *Angew. Chem. Int. Ed. Engl.* **1994**, *33*, 446−448. − [31b] C. A. Hunter, L. D. Sarson, *Angew. Chem.* **1994**, *106*, 2424−2426; *Angew. Chem. Int. Ed. Engl.* **1994**, *33*, 2313−2316.

[32] [32a] C. A. Hunter, D. H. Purvis, *Angew. Chem.* **1992**, *104*, 779−782; *Angew. Chem. Int. Ed. Engl.* **1992**, *31*, 792−795. − [32b] V. Berl, I. Huc, R. G. Khoury, M. J. Krische, J.-M. Lehn, *Nature* **2000**, *407*, 720−723. − [32c] V. Berl, M. J. Krische, I. Huc, J.-M. Lehn, M. Schmutz, *Chem. Eur. J.* **2000**, *6*, 1938−1946.

[33] Sybyl force field, Spartan, Wavefunction Inc., 18401 Von Karman Ave., Irvine, CA 92612, USA.

[34] [34a] M. Miyaura, T. Yanagi, A. Suzuki, *Synth. Commun.* **1981**, *7*, 513−519. − [34b] A. R. Katritzky, S. A. Belyakov, S. A. Henderson, P. J. Steel, *J. Org. Chem.* **1997**, *62*, 8215−8217.

[35] [35a] J. Heinze, J. Mortensen, K. Müllen, R. Schenk, *J. Chem. Soc., Chem. Commun.* **1987**, 701−703. − [35b] R. Schenk, J. Hucker, H. Hopf, H. J. Raeder, K. Müllen, *Angew. Chem.* **1989**, *101*, 942−944; *Angew. Chem. Int. Ed. Engl.* **1989**, *28*, 904−906. − [35c] K. Sandros, M. Sundahl, O. Wennerström, U. Norinder, *J. Am. Chem. Soc.* **1992**, *112*, 3082−3086.

[36] [36a] C. A. Hunter, *J. Chem. Soc., Chem. Commun.* **1991**, 749−751. − [36b] C. A. Hunter, *J. Am. Chem. Soc.* **1992**, *114*, 5303−5311. − [36c] F. Vögtle, S. Meier, R. Hoss, *Angew. Chem.* **1992**, *104*, 1628−1631; *Angew. Chem. Int. Ed. Engl.* **1992**, *31*, 1619−1622.

[37] [37a] S. Ottens-Hildebrandt, T. Schmidt, J. Harren, F. Vögtle, *Liebigs Ann.* **1995**, 1855−1860. − [37b] R. Jäger, M. Händel, K. Rissanen, F. Vögtle, *Liebigs Ann.* **1996**, 1201−1207. − [37c] F. Vögtle, R. Jäger, M. Händel, S. Ottens-Hildebrandt, W. Schmidt, *Synthesis* **1996**, 353.

[38] [38a] A. Affeld, Ph. D. Thesis, Universität Bonn, **2000**. − [38b] A. Hünten, Ph. D. Thesis, Universität Bonn, **2001**.

[39] [39a] G. M. Hübner, J. Gläser, C. Seel, F. Vögtle, *Angew. Chem.* **1999**, *111*, 395−398; *Angew. Chem. Int. Ed.* **1999**, *38*, 383−386. − [39b] C. Reuter, W. Wienand, G. M. Hübner, C. Seel, F. Vögtle, *Chem. Eur. J.* **1999**, *5*, 2692−2697. − [39c] C. Reuter, F. Vögtle, *Org. Lett.* **2000**, *2*, 593−595. − [39d] C. Seel, F. Vögtle, *Chem. Eur. J.* **2000**, *6*, 21−24.

[40] [40a] S. Ottens-Hildebrandt, S. Meier, W. Schmidt, F. Vögtle, *Angew. Chem.* **1994**, *106*, 1818−1821; *Angew. Chem. Int. Ed. Engl.* **1994**, *33*, 1767−1770. − [40b] F. Vögtle, M. Händel, S. Meier, S. Ottens-Hildebrandt, F. Ott, T. Schmidt, *Liebigs Ann.* **1995**, 739−743. − [40c] R. Jäger, T. Schmidt, D. Karbach, F. Vögtle, *Synlett* **1996**, 723. − [40d] R. Jäger, S. Baumann, M. Fischer, O. Safarowsky, M. Nieger, F. Vögtle, *Liebigs Ann./Recueil* **1997**, 2269−2273. − [40e] R. Jäger, F. Vögtle, *Angew. Chem.* **1997**, *109*, 966−980; *Angew. Chem. Int. Ed. Engl.* **1997**, *36*, 930−944.

Received February 7, 2001
[O01061]